

MEG and Neuropsychiatry

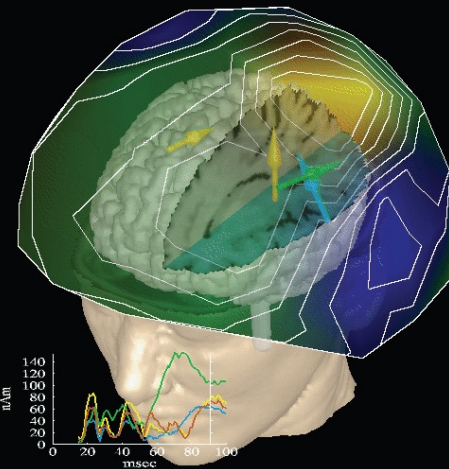
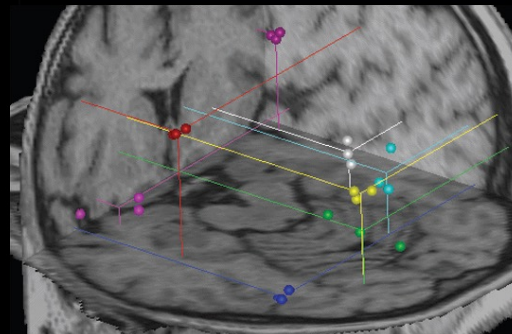
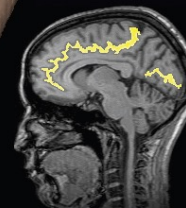
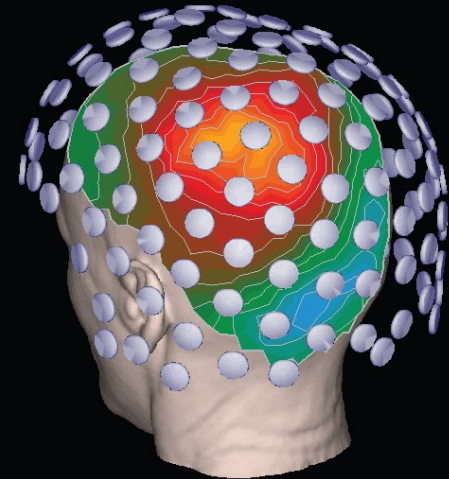
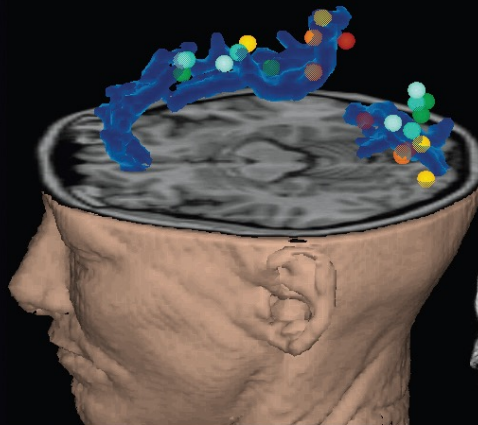
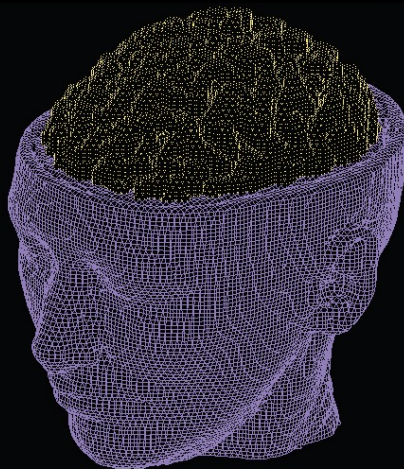
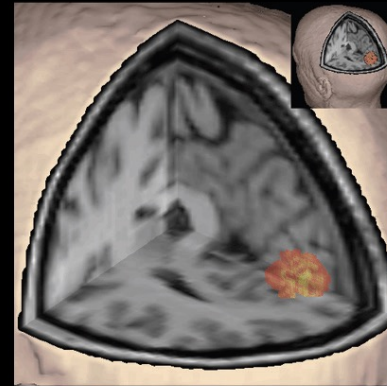
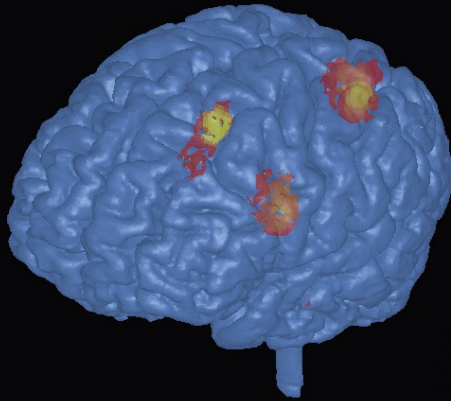
Richard Coppola, D.Sc.

NIMH MEG Core Facility

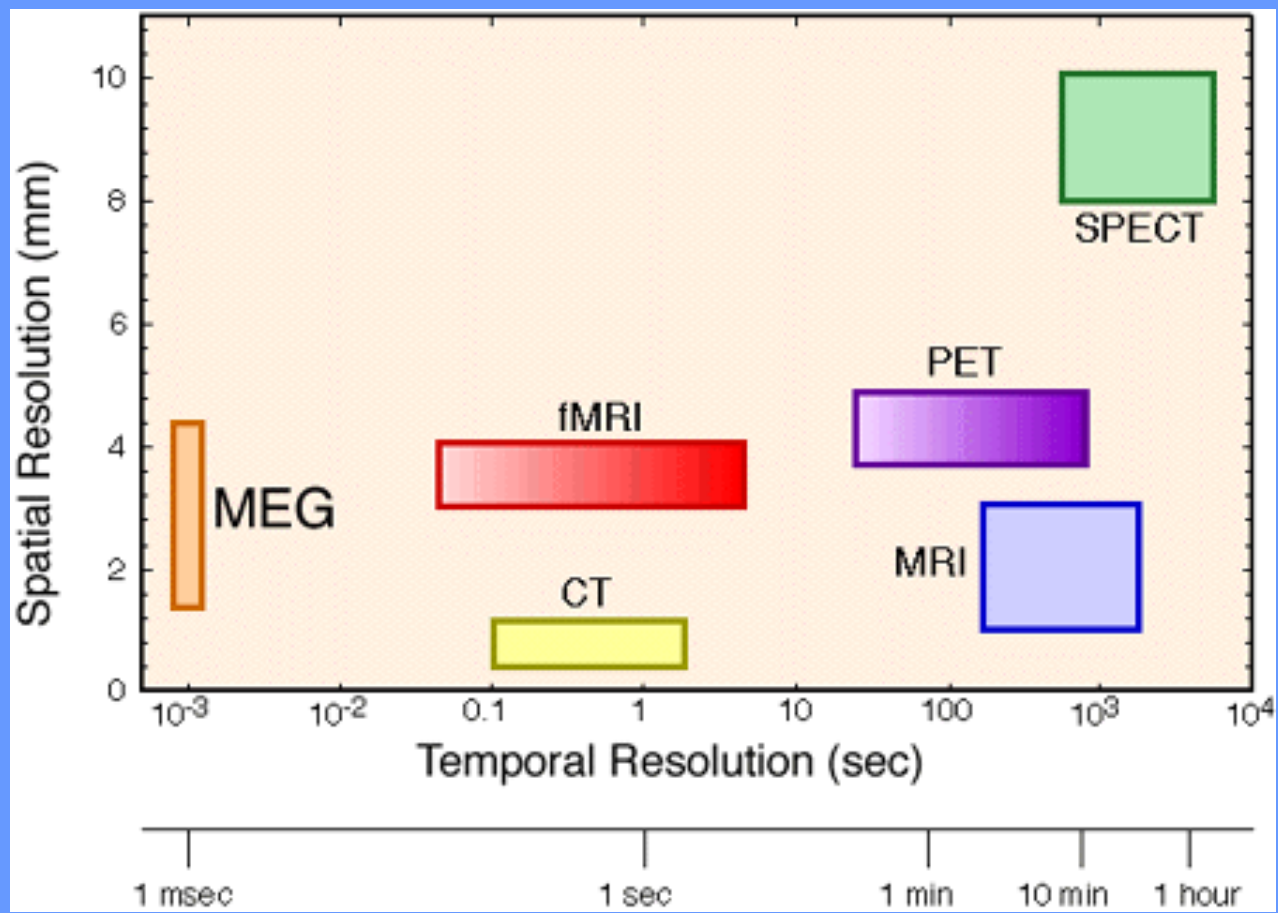


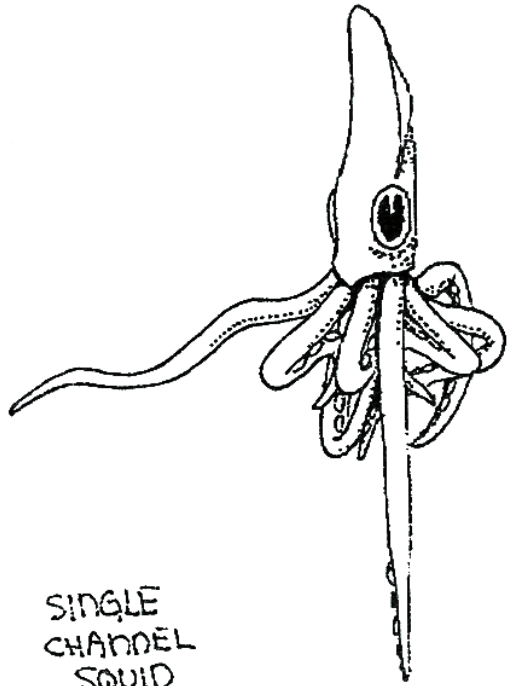
NIMH
National Institute
of Mental Health





Piše/By **Davorka Vukov-ColiĀ**
Slike/Images **Douglas Ranken**

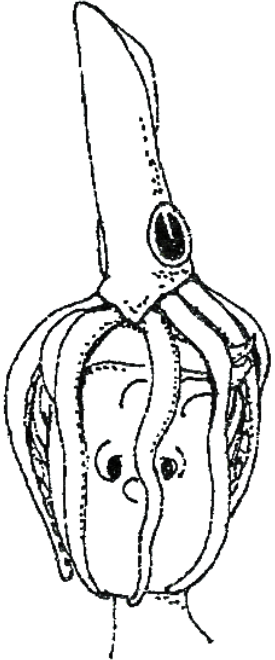




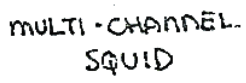
SINGLE
CHANNEL
SQUID



EIGHT
CHANNEL
SQUID



MULTI-CHANNEL
SQUID



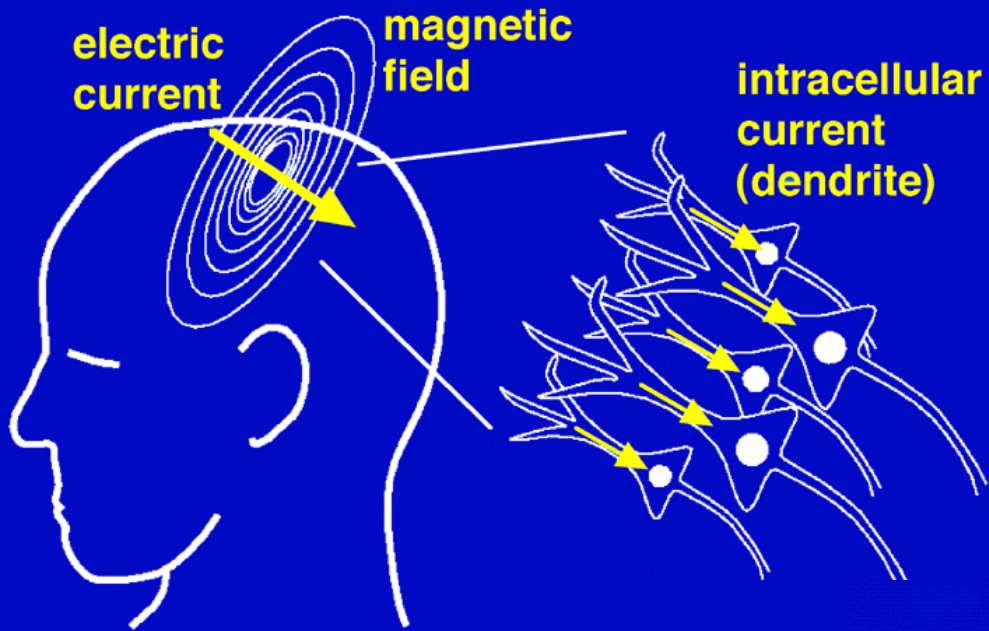


MEG

Functional Imaging



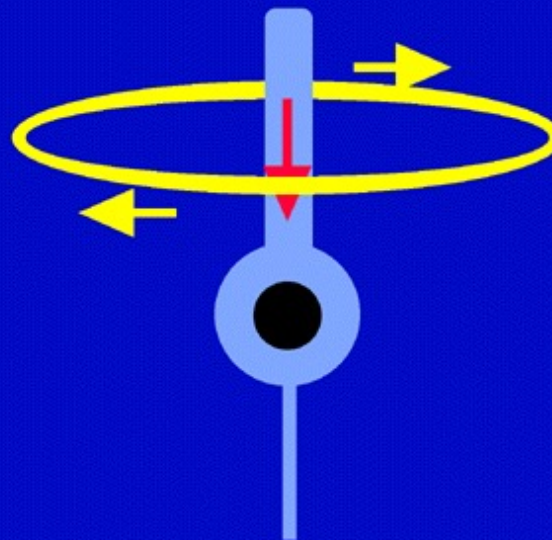
The visual stimuli are projected on a screen



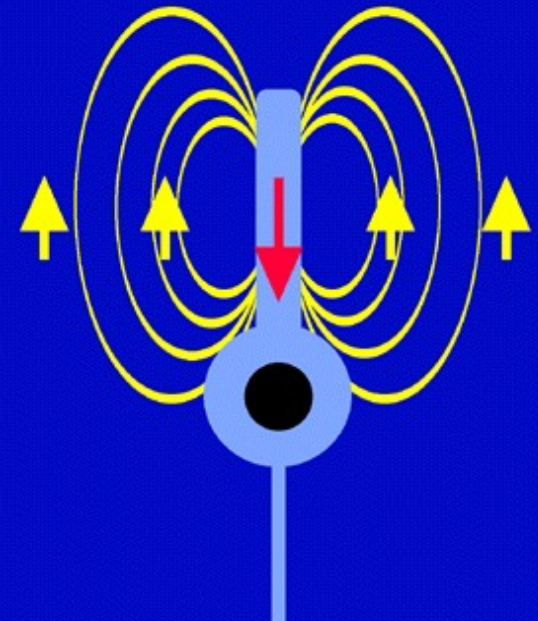
A close group of neurons can act as a single current source, which in turn gives rise to a magnetic field over the surface of the head.

MEG's primary response is to tangential fields, whereas EEG can be used to measure radial fields. Furthermore, MEG measures intercellular current while EEG measures volume extracellular currents. The information that is contained with these two measures is complementary.

MEG:
intracellular
current



EEG:
extracellular
current



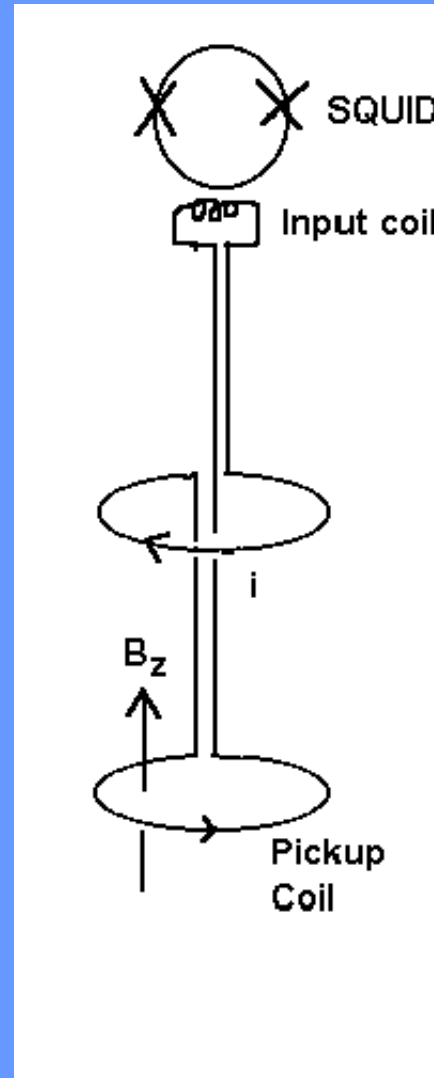
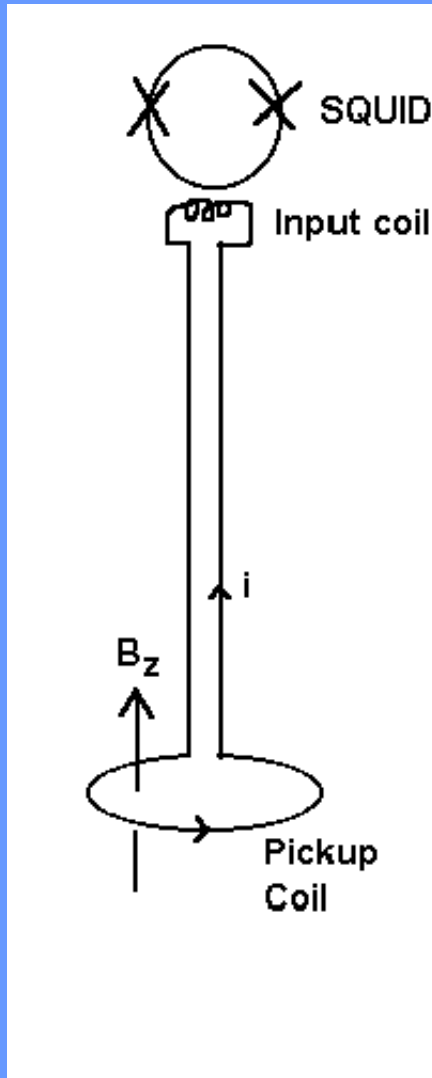
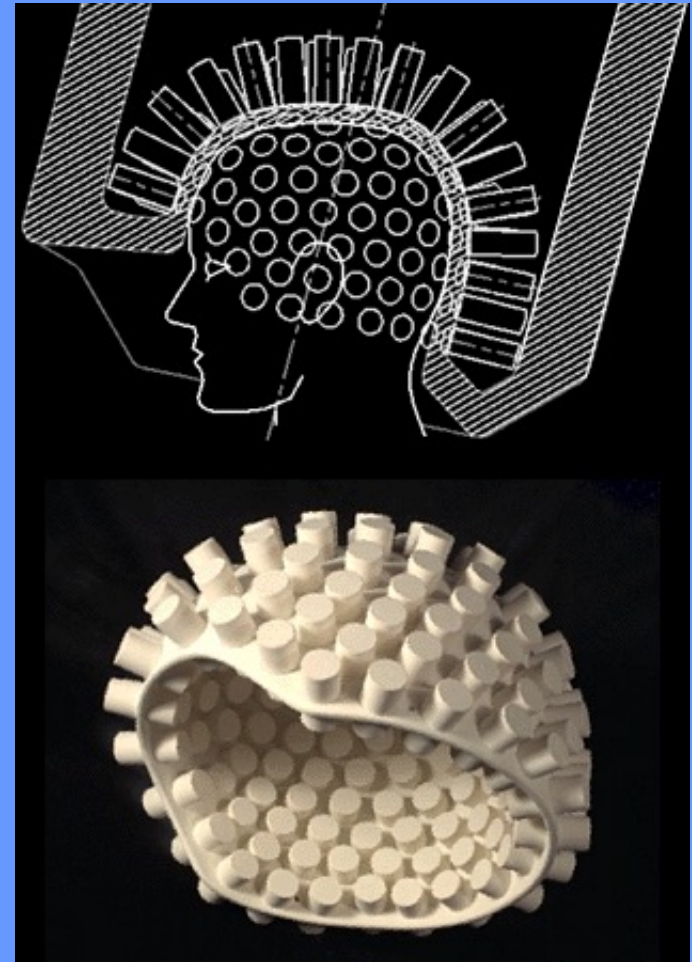
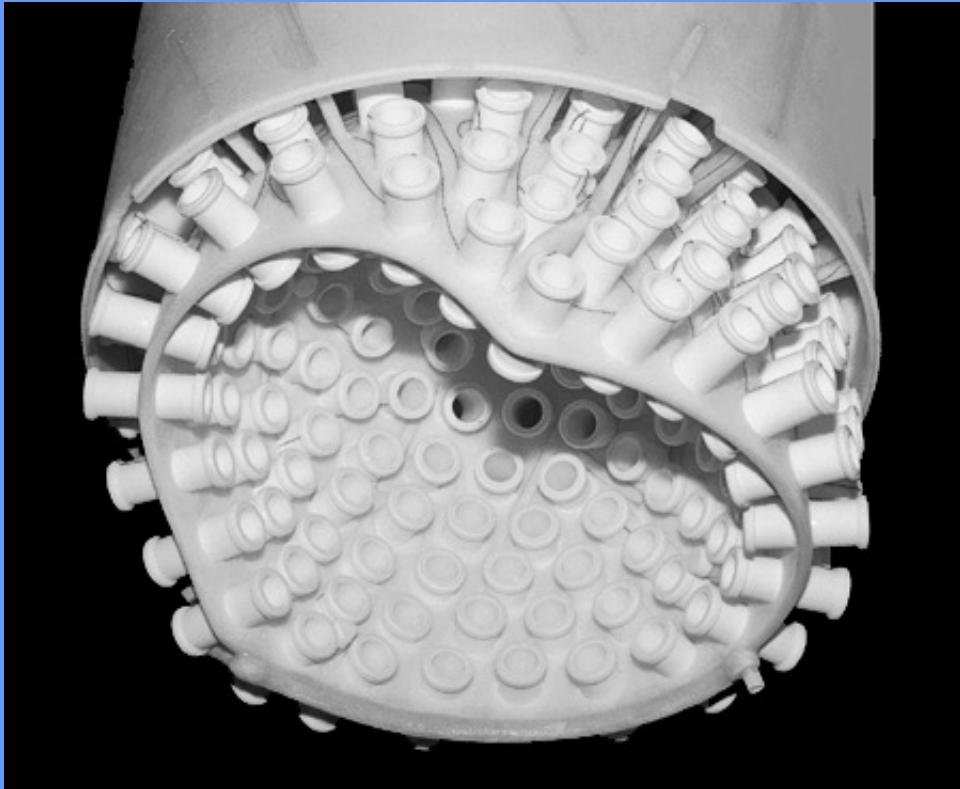


Figure 2. Flux transformers used to transport flux to the SQUID loop.

(a) shows a simple one coil flux transformer; (b) a first order gradiometer.



CTF 151 Channel array

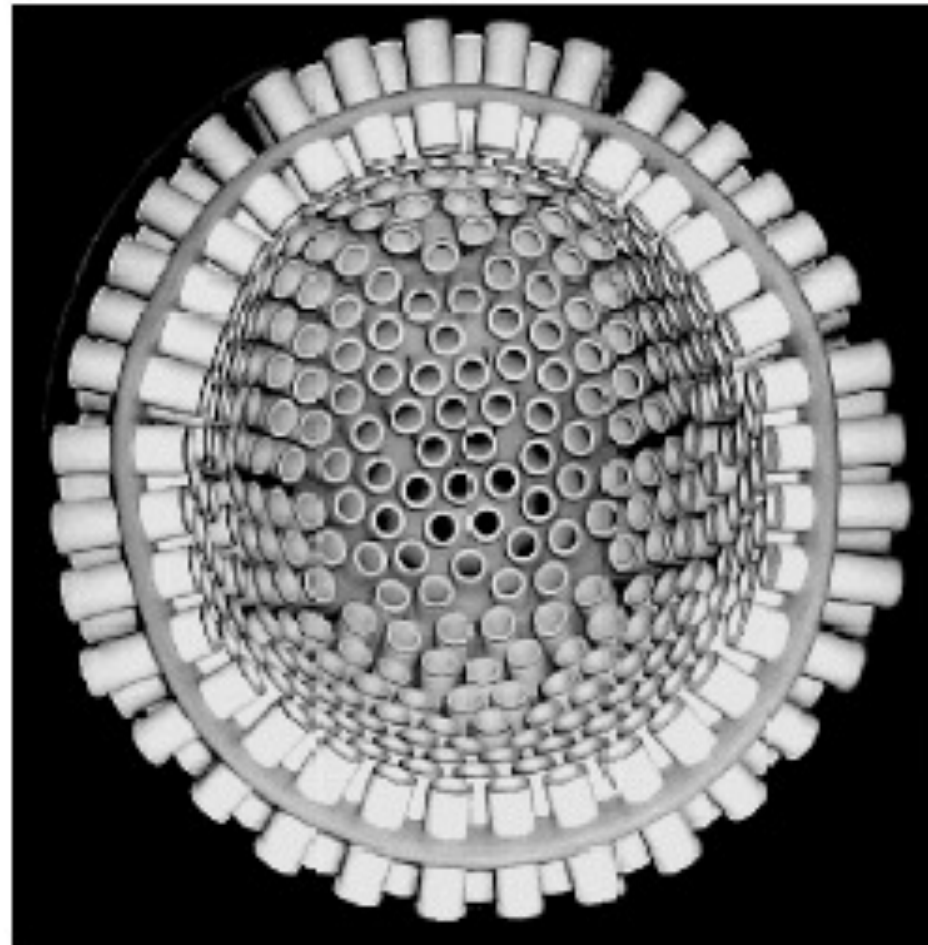
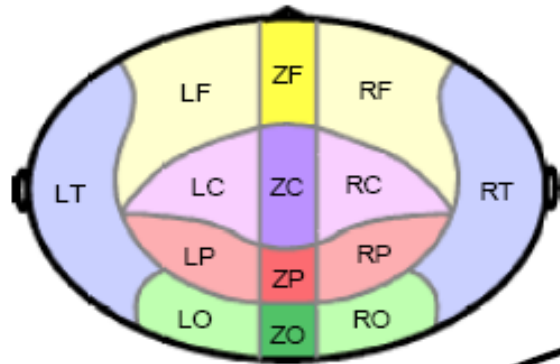


Fig. 2 End (axial) view of the 275-channel MEG sensor array showing 275 radial 1st gradiometers with optimized baselines $b_1 = 50$ mm and coil diameters = 18 mm, mounted in a rigid helmet-shaped support.

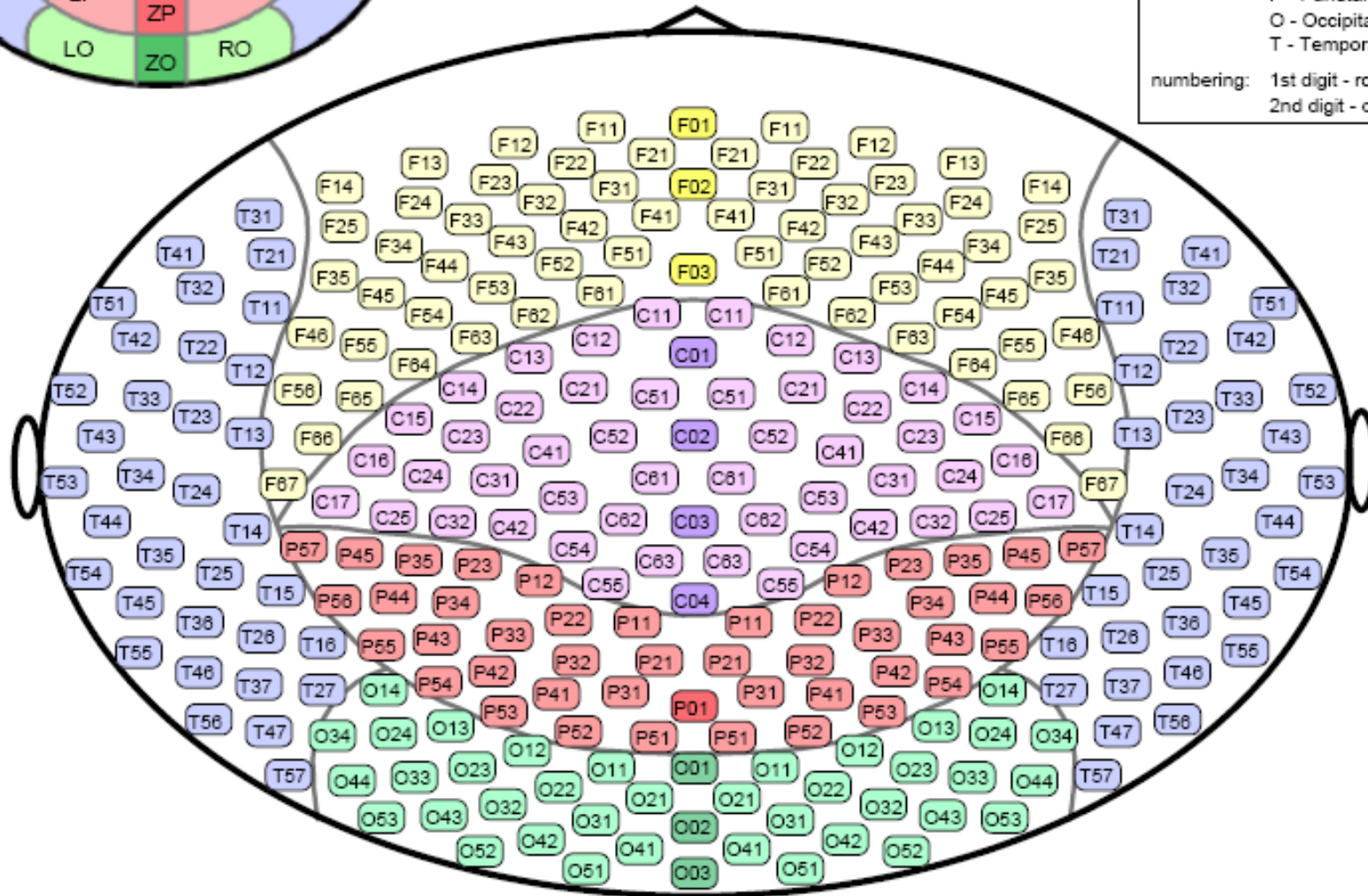
Sensor Names - 275 Channel Systems



CHANNEL COUNT:

	Frontal	Central	Parietal	Occipital	Temporal	Totals
Z (Midline)	3	4	1	3	0	11
L (Left)	33	24	22	19	34	132
R (Right)	33	24	22	19	34	132
Totals	69	52	45	41	68	275

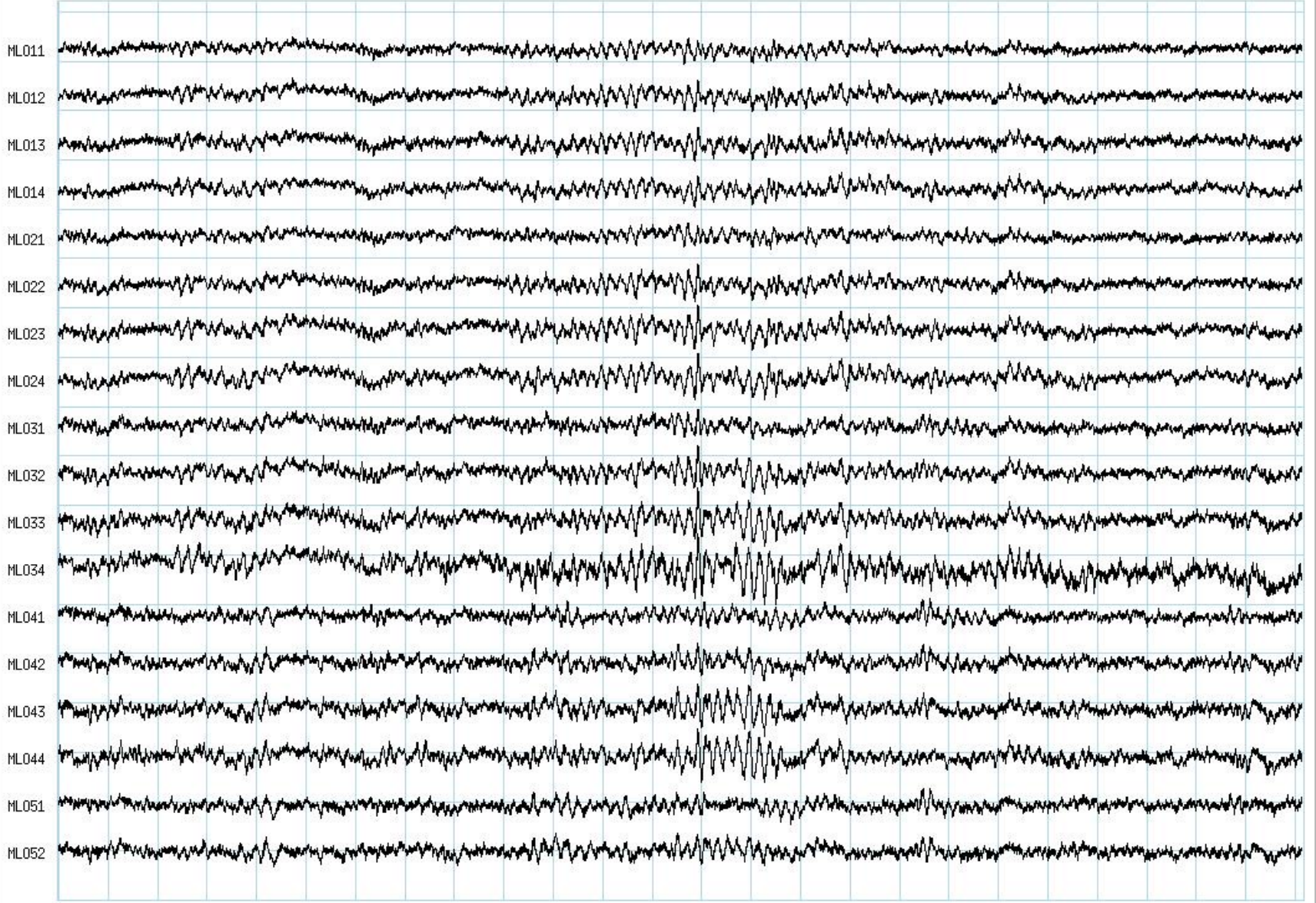
- 1st letter: M - MEG
E - EEG
- 2nd letter: L - Left
R - Right
Z - Zenith (midline)
- 3rd letter: F - Frontal
C - Central
P - Parietal
O - Occipital
T - Temporal
- numbering: 1st digit - row
2nd digit - column





Set Trial Class Edit Markers

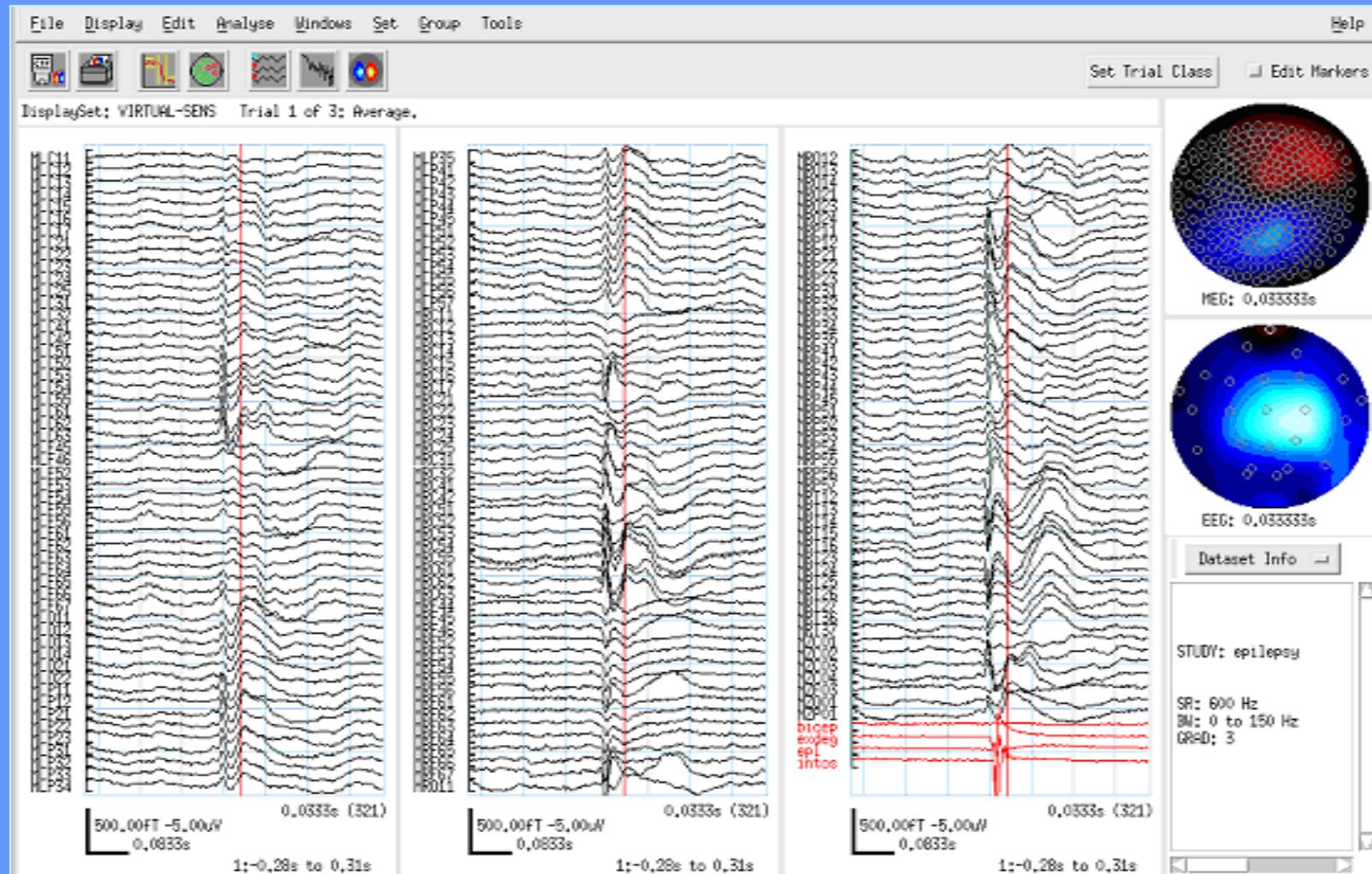
DisplaySet: None Trial 7 of 16: Unclassified.



7:0.00s to 12.58s

Time Scale: 0.5000 sec/cm Gain: MEG-SENS 2p T/div
Marker: None Go to... I<< >>I

MEG example



Epileptic spike associated with muscle twitch



Coils for measuring head position
attached at anatomical landmarks

File Options Tools Help

Slice: 125 of 256 (Coronal) Anterior Posterior
 Slice: 127 of 256 (Sagittal) Left Right
 Slice: 125 of 256 (Axial) Superior Inferior

Lock views to cursors
 Goto: Nasion Right Ear
 Left Ear Sphere Origin

Sphere:
 R(cm) X(cm) Y(cm) Z(cm)
 9.31 -1.56 0.27 4.57

Dipole:
 of 100
none none
 Show all in this slice
 Show all
 Selected Only Hide bad

Markers:
 of 0

CTF Systems Inc

File Options Tools Help

Slice: 86 of 256 (Coronal) Anterior Posterior
 Slice: 196 of 256 (Sagittal) Left Right
 Slice: 148 of 256 (Axial) Superior Inferior

sag= 196, cor= 86, axi= 148 (voxels)
 x= 3.84, y= -6.47, z= 3.00 (cm)

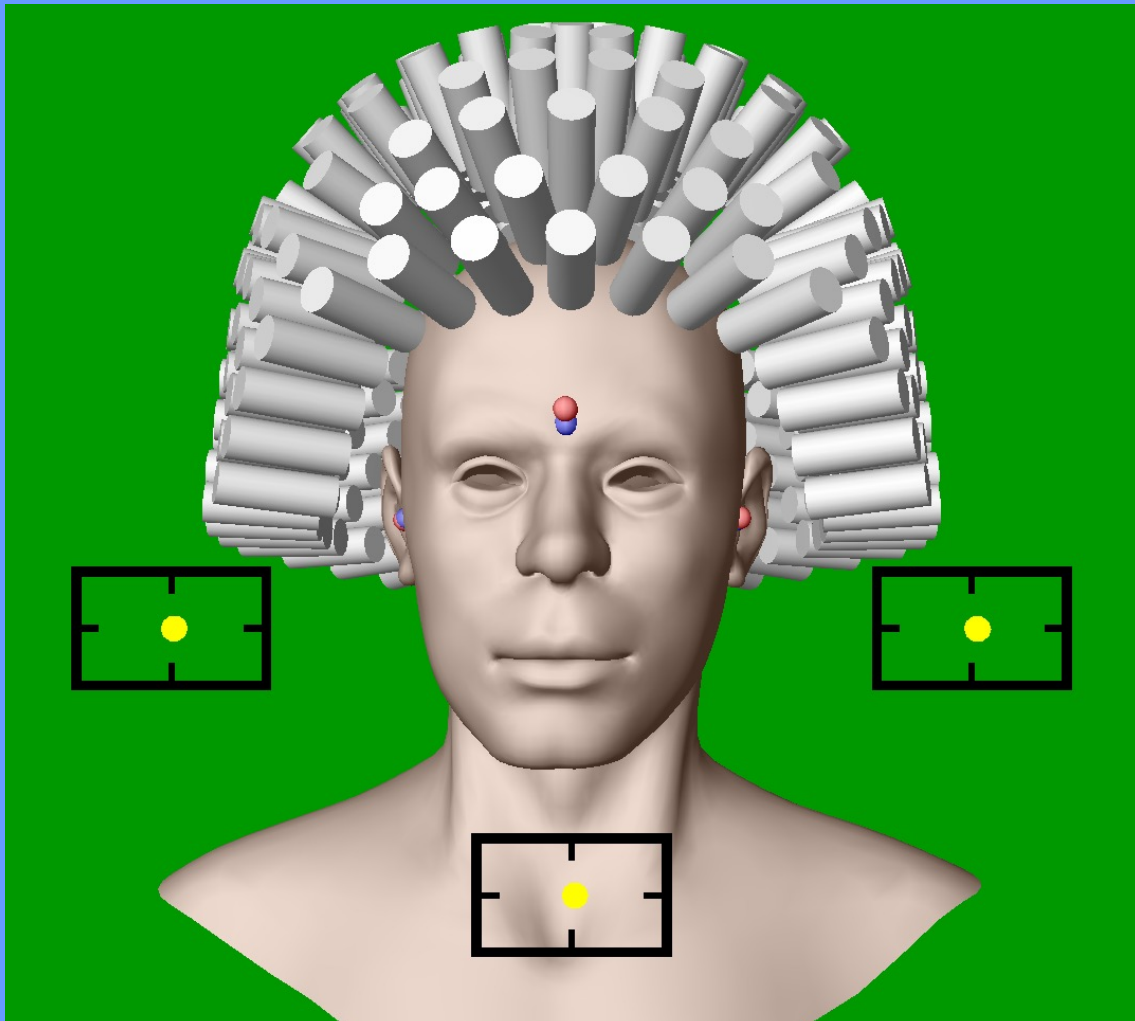
Lock views to cursors
 Goto: Nasion Right Ear
 Left Ear Sphere Origin

Sphere:
 R(cm) X(cm) Y(cm) Z(cm)
 9.31 -1.56 0.27 4.57

Dipole:
 of 100
none none
 Show all in this slice
 Show all
 Selected Only Hide bad

Markers:
 of 0

CTF Systems Inc



Target boxes indicate current position relative to previous head localization

Development Project: RealTime Head Localization display

Facilitates repositioning subject in helmet

Time Series Analysis

- What are we looking for?
 - Individual spikes or complex waveforms
 - Oscillations at particular frequency bands e.g. theta (4-8Hz), alpha (8-13Hz), beta (14-30Hz), gamma (30-50Hz)
- Magnetoencephalogram (MEG)
 - Raw time series unrelated to a stimulus
 - e.g. epileptic spikes / sleep stages
- Evoked Fields
 - Time series averaged around an event
 - Generic early sensory or motor responses
- Event-related Fields (ERFs)
 - Late cognitive responses (>150ms)
 - Vary depending on experimental context

Source Analysis Techniques (two of many)

– Dipole Fits

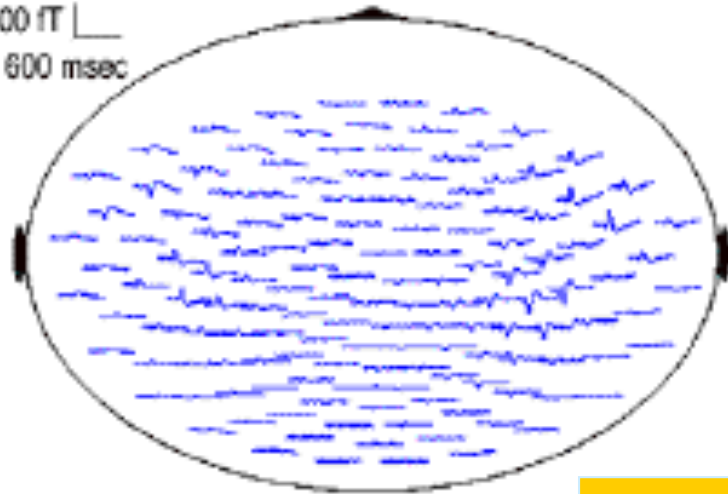
- Used to find one or a few focal sources
- Best for primary sensorimotor evoked fields

– SAM (synthetic aperture magnetometry)

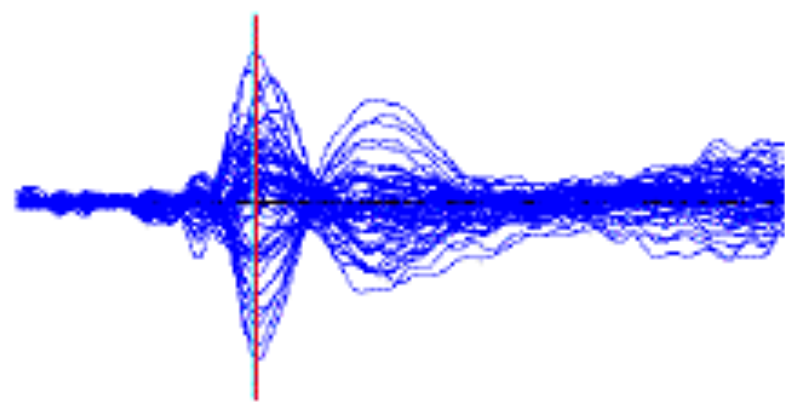
- Produces whole brain estimates of source power for specified frequency bands
- Best for cognitive event-related experiments

Dipole Fit

800 fT
600 msec

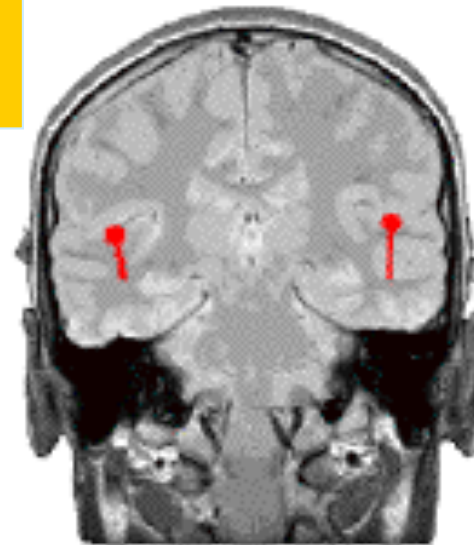
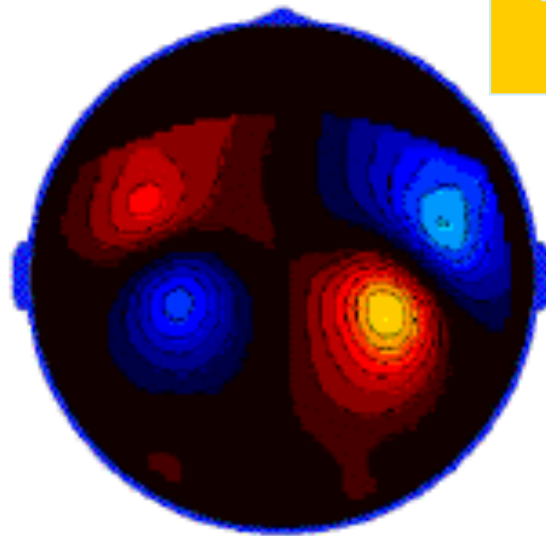
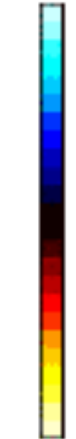


97 msec



Auditory
N100m

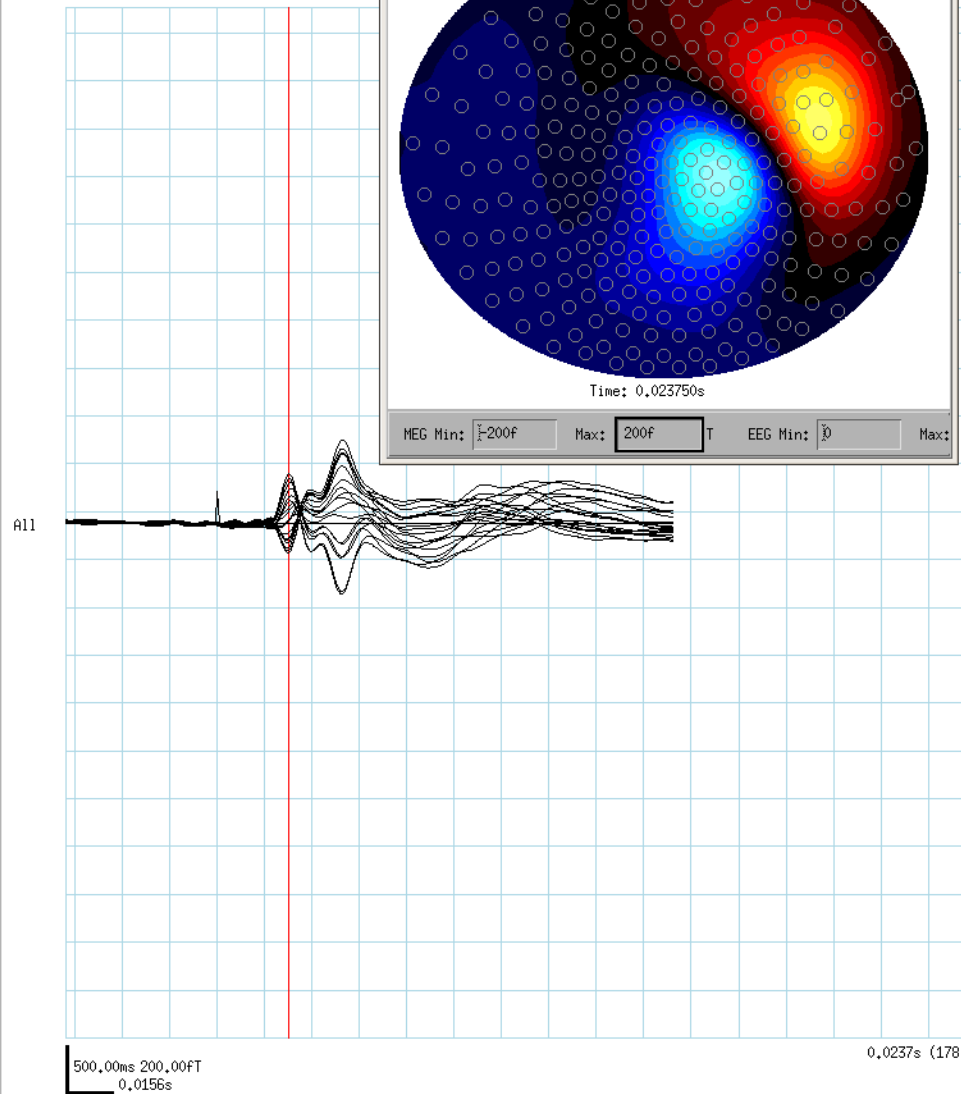
360 fT



File Display Edit Analyse Windows Set

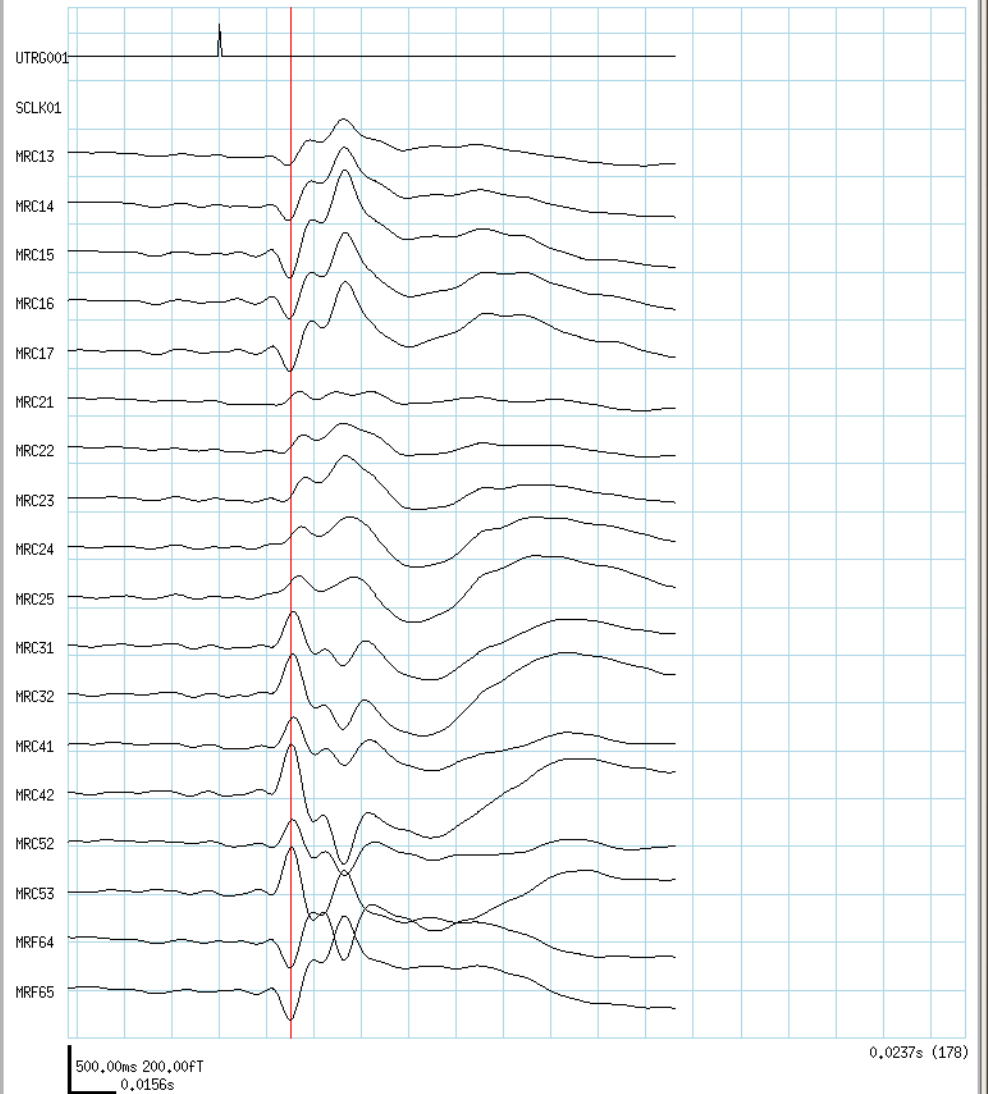


ChannelSet: MEG-REF Trial 1 of 3: Average.



Help

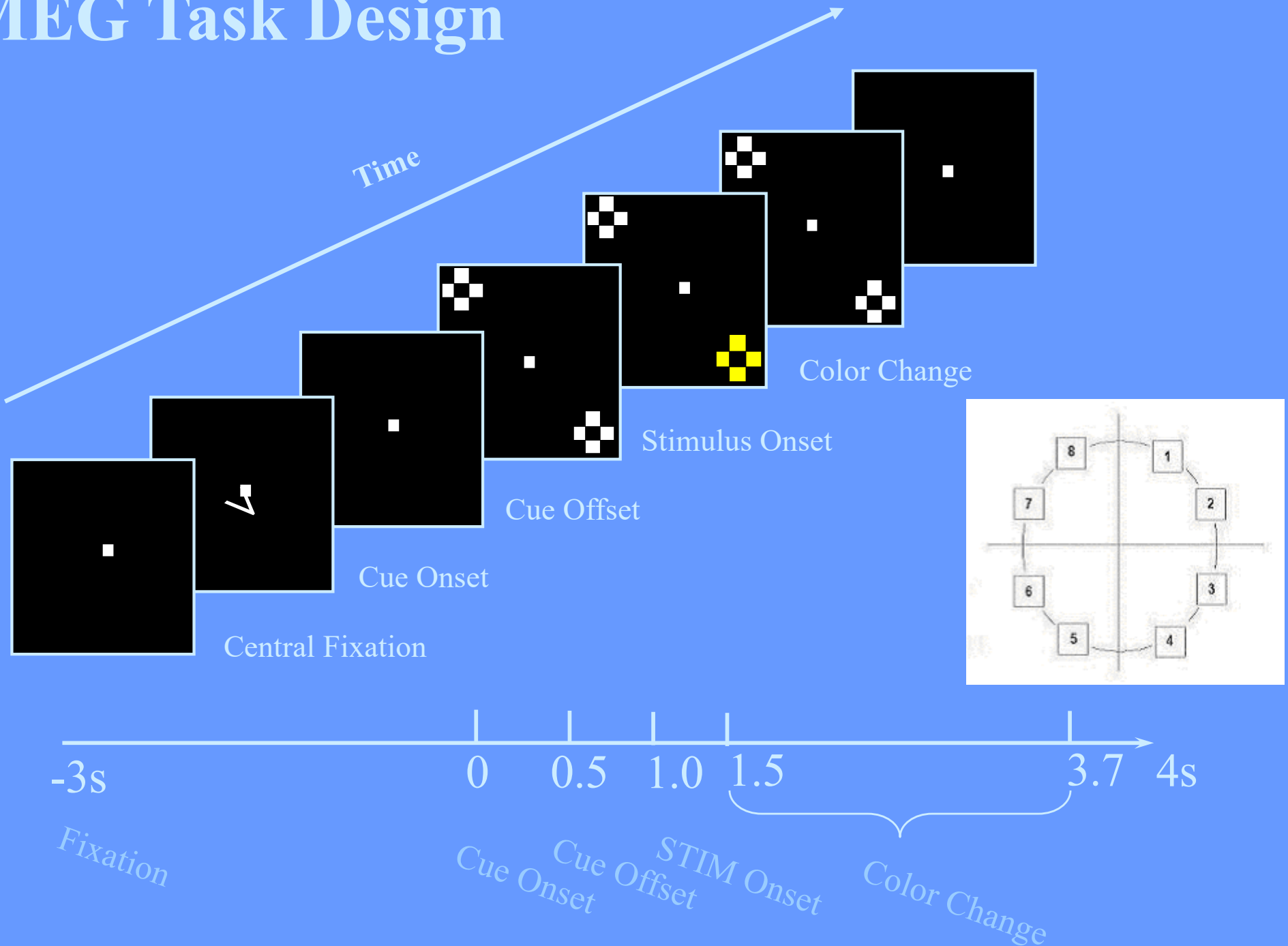
Set Trial Class Edit Markers



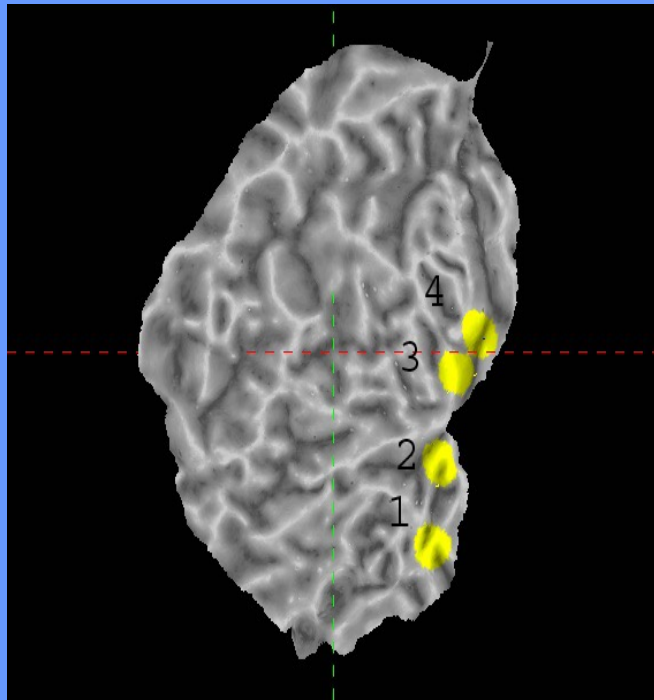
Time Scale: 40.0000 mm/sec Gain: STIM-REF 100k /div

Marker: None Go to... <<>>

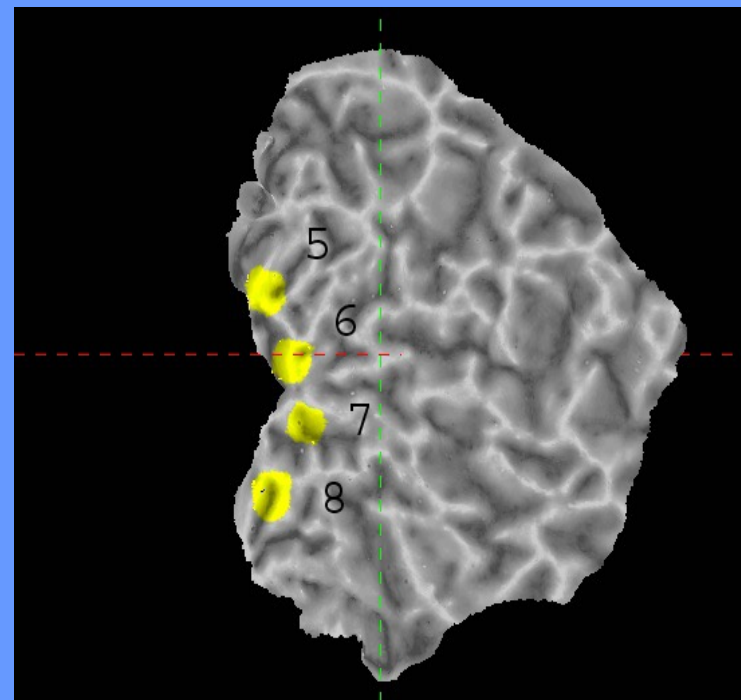
MEG Task Design



DipoleFit for 7.5Hz Flicker

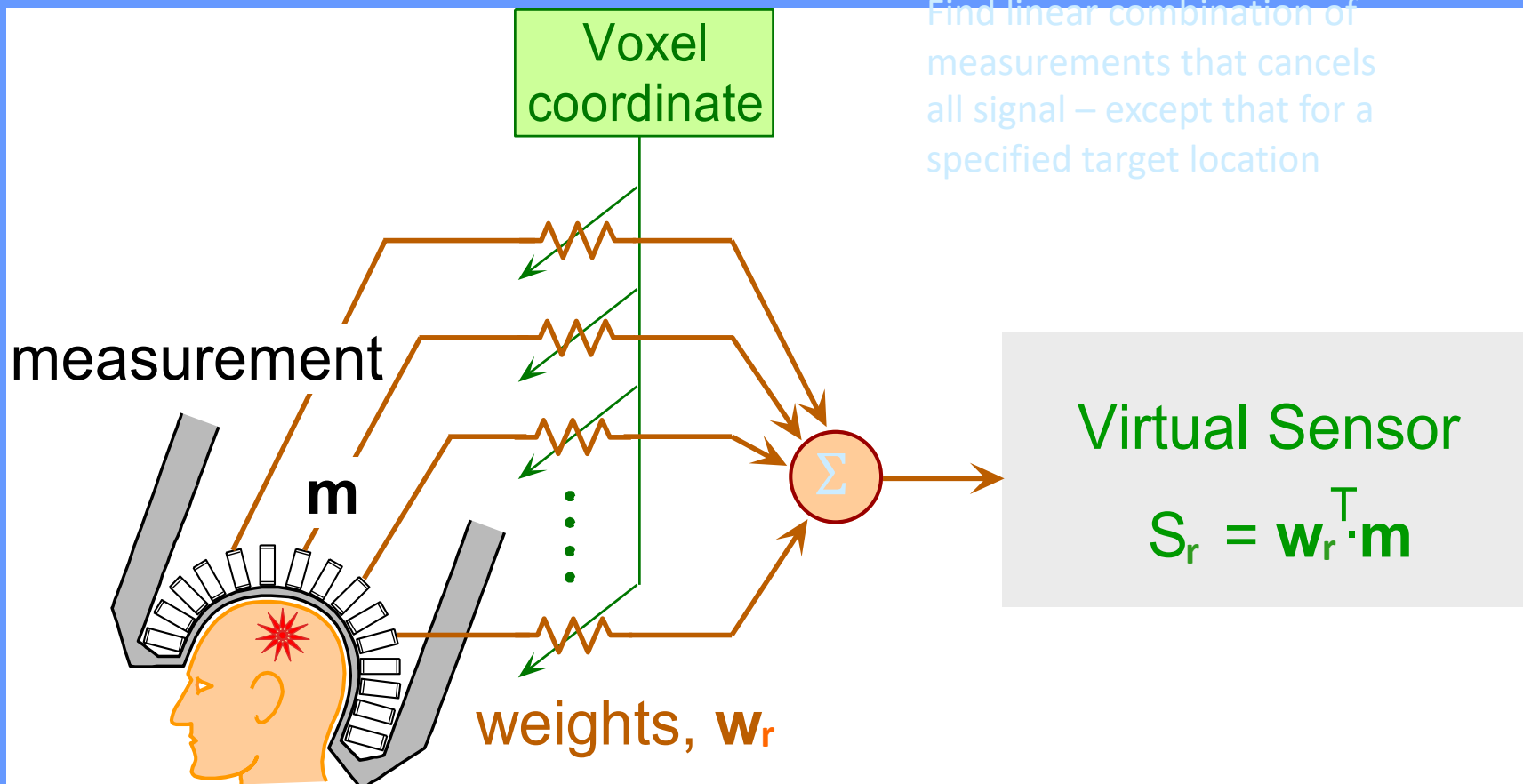


Left Hemisphere



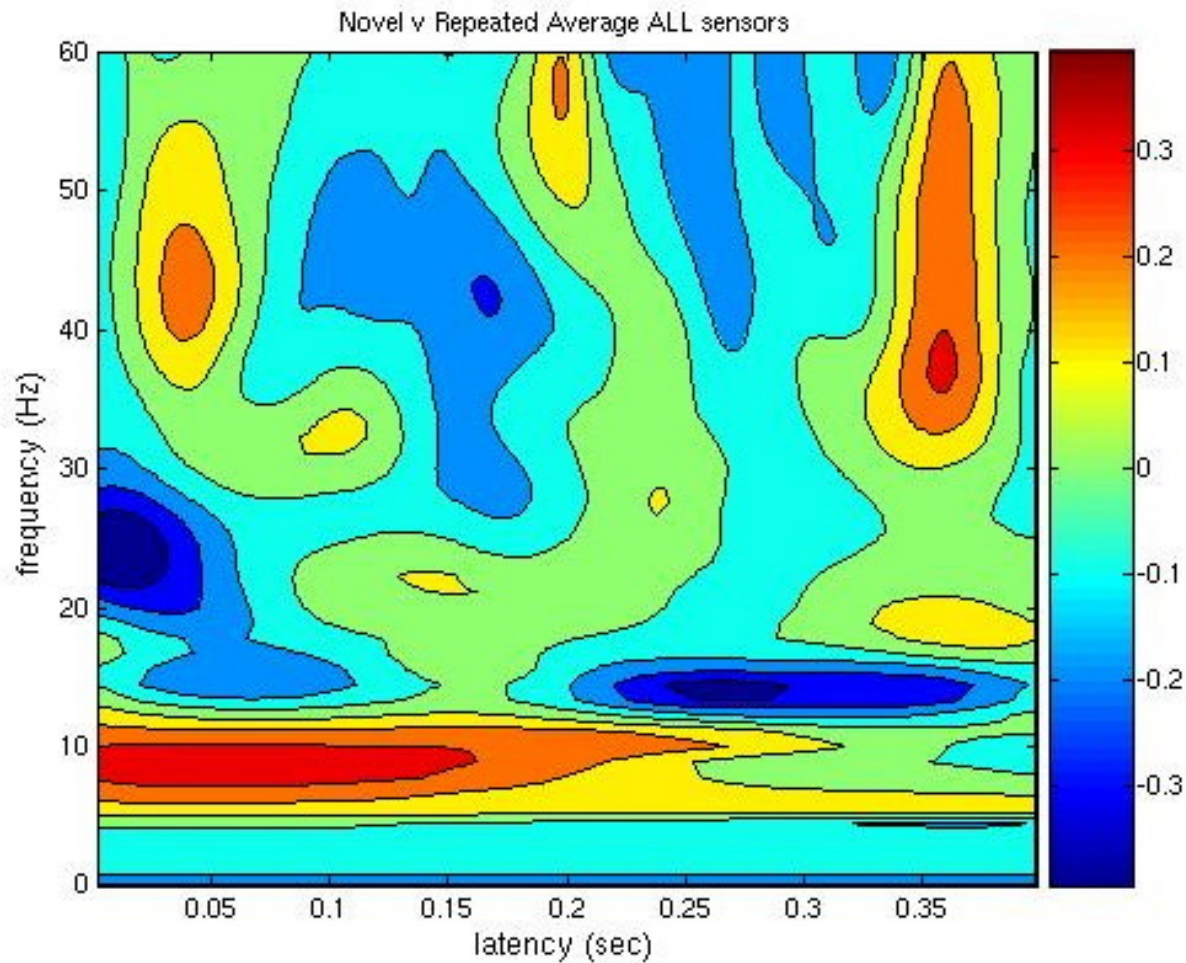
Right Hemisphere

SAM Beamformer Principle

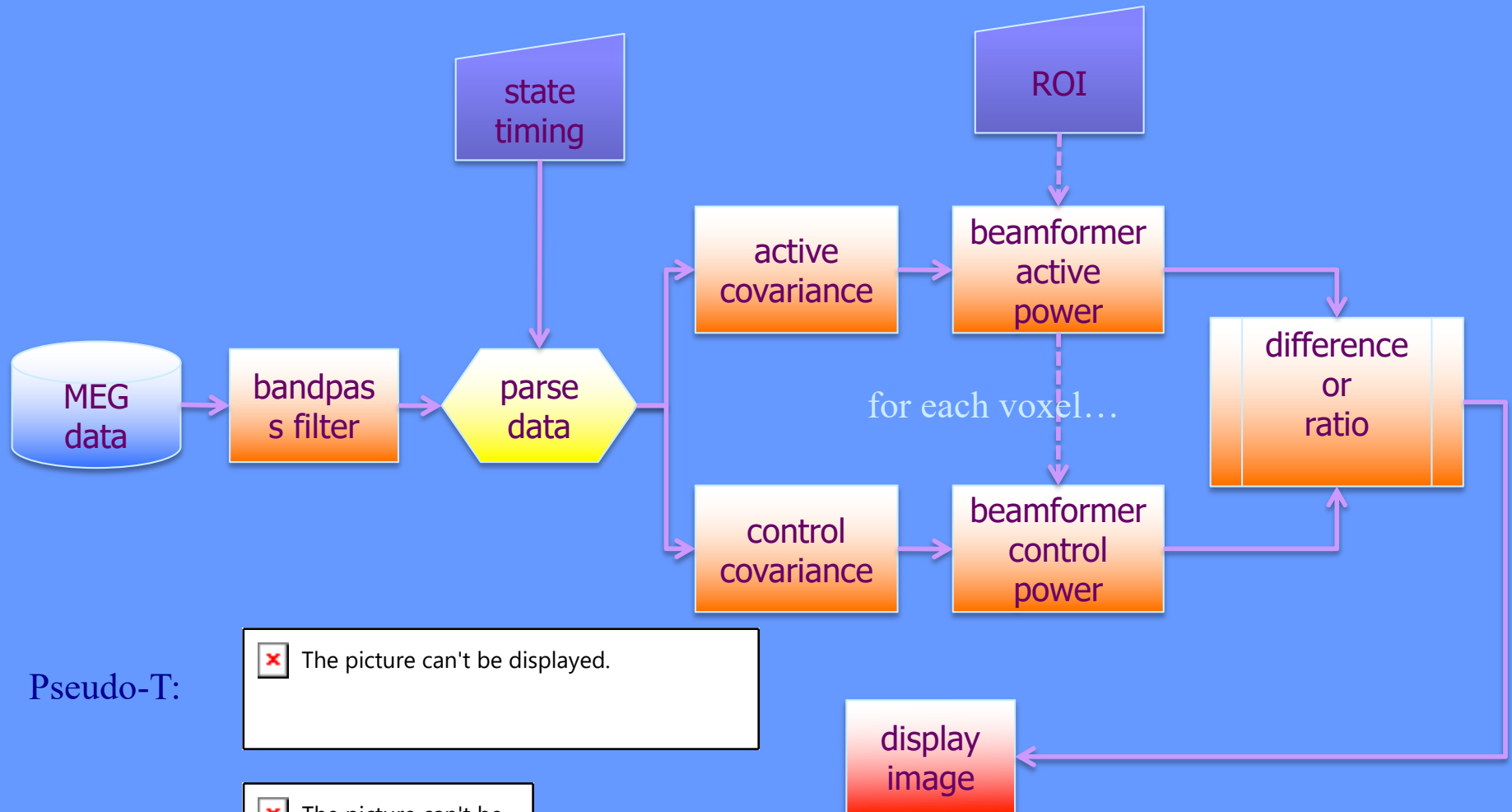


Time-Frequency (Stockwell): Evoked Components

Novel vs Repeated



Dual-State Beamformer Imaging using SAMimg

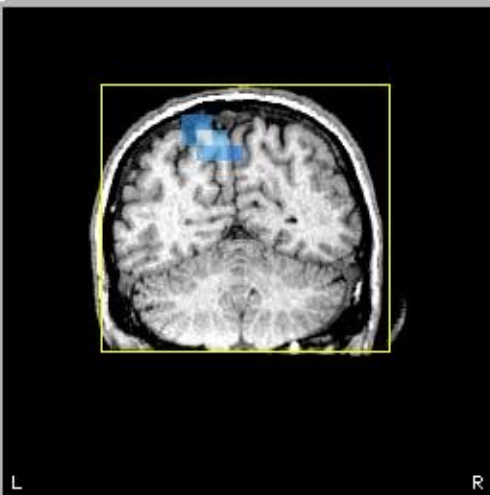


Pseudo-T:

The picture can't be displayed.

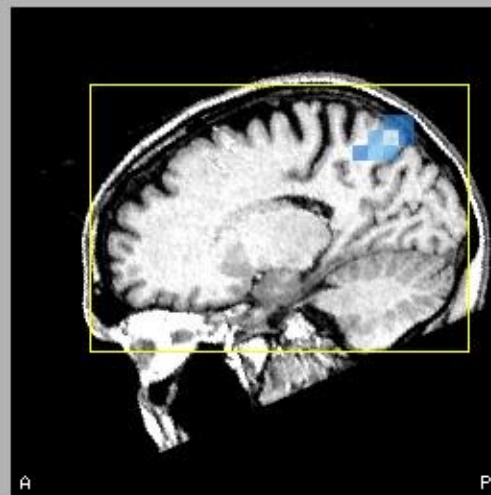
Pseudo-F:

The picture can't be displayed.



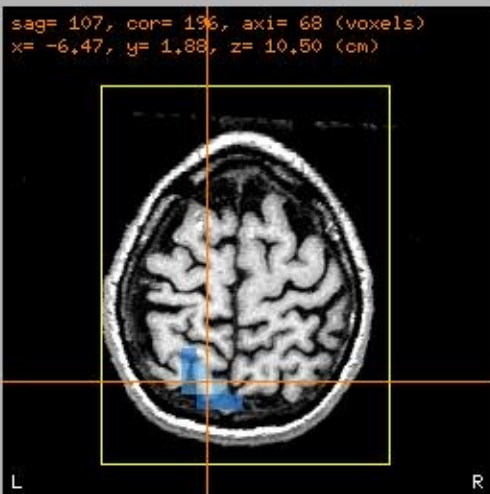
Slice: 196 of 256
(Coronal)

Anterior Posterior



Slice: 107 of 256
(Sagittal)

Left Right



Slice: 68 of 256
(Axial)

Superior Inferior



SAM Settings

Lock views to cursors

Goto: Nasion Right Ear
 Left Ear Sphere Origin

Sphere:

R(cm)	X(cm)	Y(cm)	Z(cm)
9.31	-1.56	0.27	4.57

Dipole:

of 100

none

none

Show all in this slice

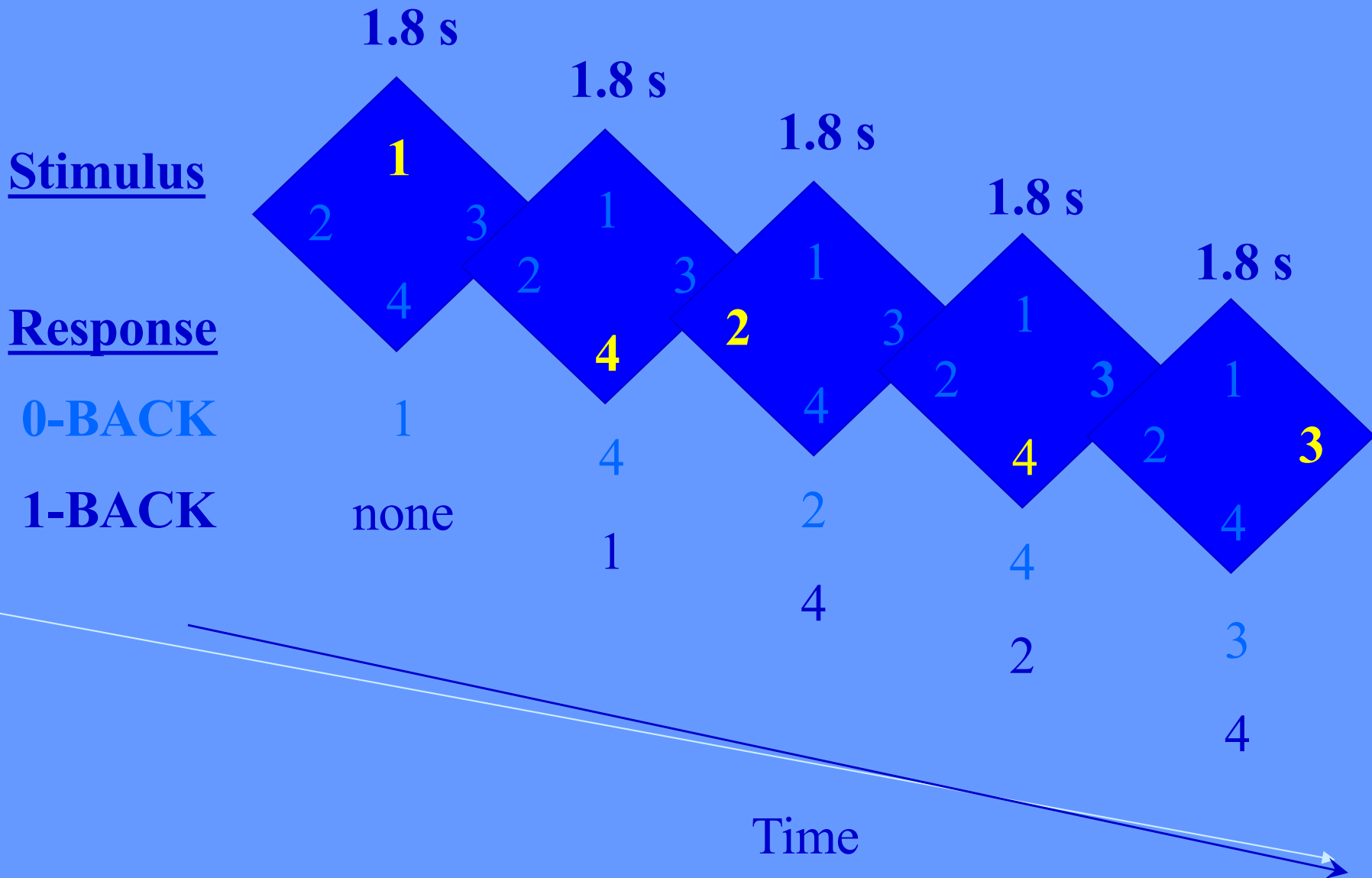
Show all

Selected Only Hide bad

Markers:

of 17

Methods: N-Back Task





DataEditor window with marks in the stimulus and ADC channels

Task Details

- Sixteen 22 sec blocks of alternating 0-back and 2-back
- Stim: one of four numbers (0.5 duration, 1.8 sec ITI)
- normal volunteers strongly right handed
- 2-back accuracy greater than 65%

Data Analysis

- SAM: Synthetic Aperture Magnetometry
- Optimum spatial filter for each .75 cm voxel calculated from dual state freq domain covariance matrix
- Time windows:block(14 sec), stim (500 msec), resp (500 msec)
- Theta, alpha, beta, gamma, freq bands
- Group 3d map from Talairach aligned volumes using AFNI, n=18 NC
- Blue=desynch; Red=power increase

Group Analysis

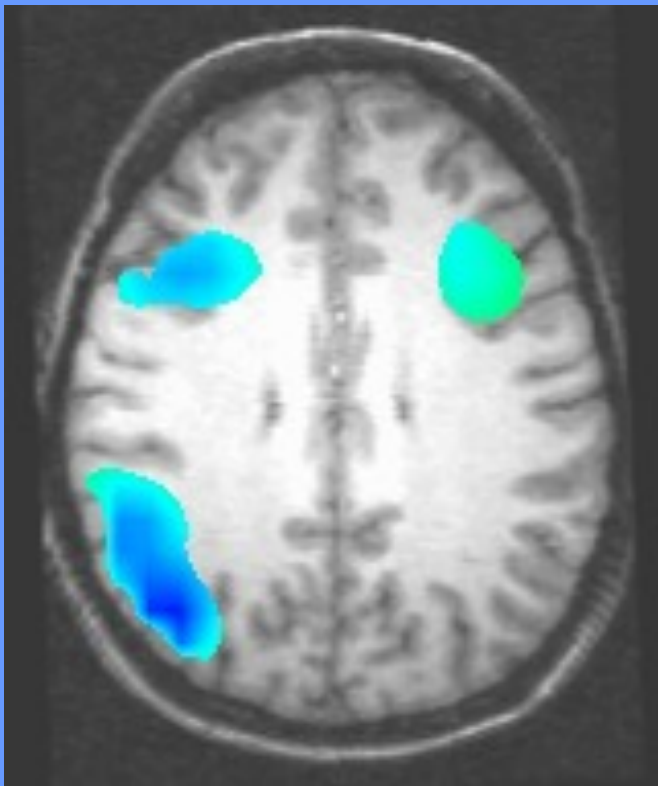
- MRI's Talairach aligned in AFNI
- SAM image z-score normalized by pooled variance
- AFNI 3dmean averaged warped SAM volumes
- Normalized t statistic (3dttest) to threshold group mean map

fMRI Processing

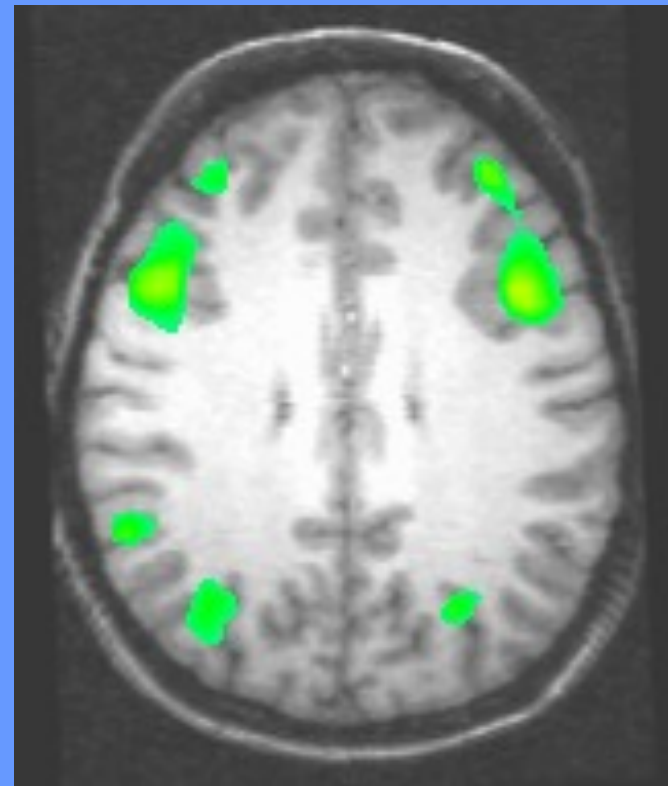
- 3T GE EPI-RT, 24 slices, TE 30, TR 2000, FOV 24 cm, voxel 3.75x3.75x6 mm, 64 x 64 matrix
- Structurally aligned, smoothed and normalized to MNI space, SPM99
- Single subj block design contrast for 2back > 0back
- Group second level analysis at approx $p > .001$

MEG and fMRI

2-back vs 0-back memory task, Block design
same 12 subjects, group map at p approx $<.001$



SAM 500 msec window on
response, Beta desynchronization



SPM T map 2b>0b {SPM99 $t \sim$
4.0; $Z_{\equiv} \sim 3.10$, $p \sim 0.001$, $k > 10$ }

CBDB and NIMH MEG Core



[A]u AFNI: ./SUMA_beta/colinN27+tlrc & volume+tlrc



[order: RAI=DICOM]
 x = -39.000 mm [R]
 y = -7.000 mm [A]
 z = 27.000 mm [S]

Xhairs Multi X+
 Color green
 Gap 5 Wrap
 Index

Axial Image Graph
 Sagittal Image Graph
 Coronal Image Graph

Original View
 AC-PC Aligned
 Talairach View

Define Overlay ->
 See Overlay

Define Datamode ->

DataDir Switch Read

UnderLay EditEnv
 OverLay NIML+P0
 Control Surface

s[0] Inten Background Clusters

bkgd:ULay Clusterize
 bkgd:OLay *Clear Rpt

ULay #0 Colins brain
 Olay #0 c[0]
 Thr #1 s[0]

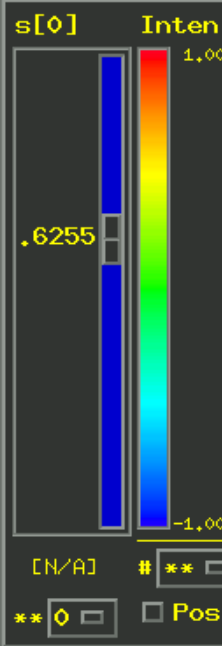
ULay 0: 152.0023
 Olay -0.092747: 1.476897
 Thr -0.728336: 10.85913

autoRange: 1.476897
 Rota

See TT Atlas Regions

ULay = 76.00116
 Olay = 0.848466
 Thr = 5.808047

Pos?



[A]u AFNI: ./SUMA_beta/colinN27

92

Axial: left=Left float [2%-98%]

Disp Sav1.ppm Mont Done Rec



[A]u AFNI: COMT_NC_Beta_2vs0/IAUPZIDG_20040330/link to N27_SurfVol+tlrc & resp2vs0,14-30H:

[A]u AFNI: COMT_NC_Beta_2vs0/

menu

Quit

+++++++ nearby Atlas structures ++++++

Focus point (LPI)=
 40 mm [R], 13 mm [A], 27 mm [S] {T-T Atlas}
 40 mm [R], 12 mm [A], 30 mm [S] {MNI Brain}
 42 mm [R], 14 mm [A], 30 mm [S] {MNI Anat.}

Atlas TT_Daemon: Talairach-Tournoux Atlas
 Focus point: Right Middle Frontal Gyrus
 Within 3 mm: Right Inferior Frontal Gyrus
 Within 4 mm: Right Brodmann area 9
 Within 7 mm: Right Precentral Gyrus
 -AND- Right Brodmann area 46

Atlas CA_N27_MPM: Cytoarch. Max. Prob. Maps (N27)
 Within 4 mm: Area 45
 Within 6 mm: Area 44

Atlas CA_N27_ML: Macro Labels (N27)
 Focus point: Right Inferior Frontal Gyrus (p. Triangularis)
 Within 2 mm: Right Inferior Frontal Gyrus (p. Opercularis)

Clusters

Clusterize
 *Clear Rpt

#0
 #0
 #0

0: 253
 941249: 0.374406
 941249: 0.374406

ange: 0.941249

Rota

Atlas Regions

2
 0.341648
 0.341648

92

Axial: left=Left byte [2%-98%]

Disp Sav1.ppm Mont Done Rec

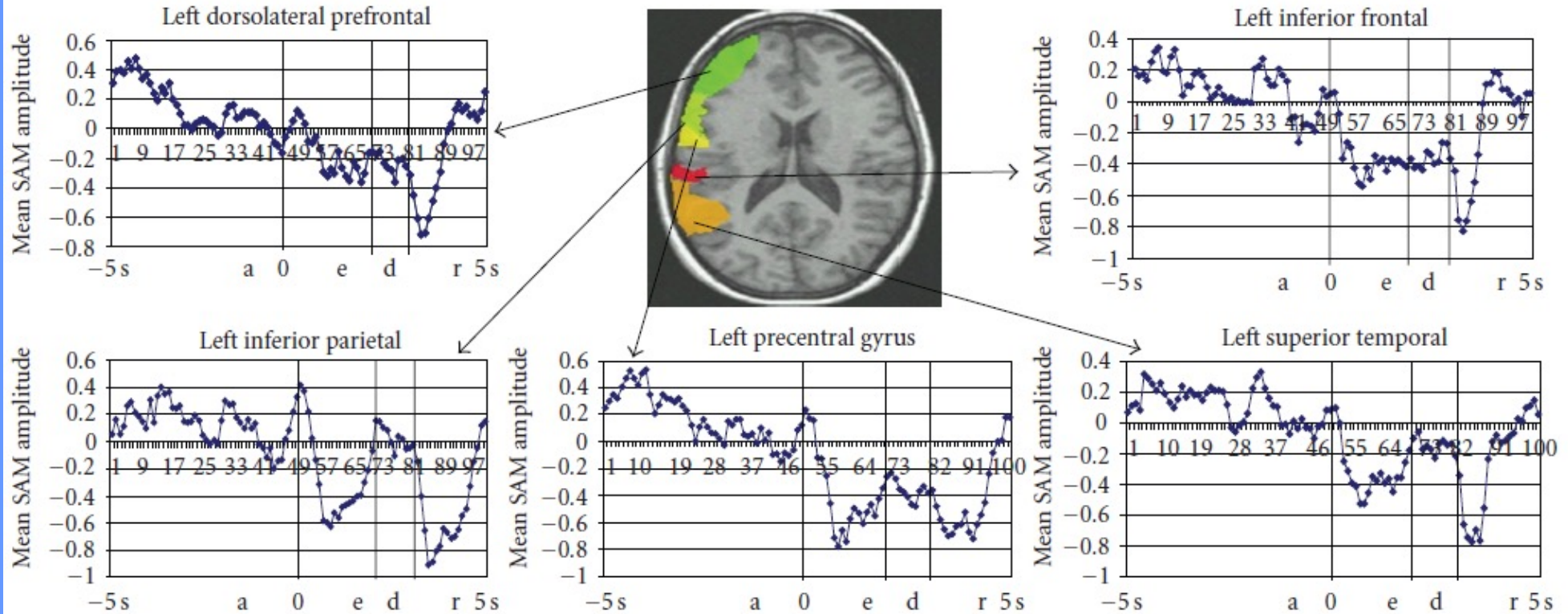
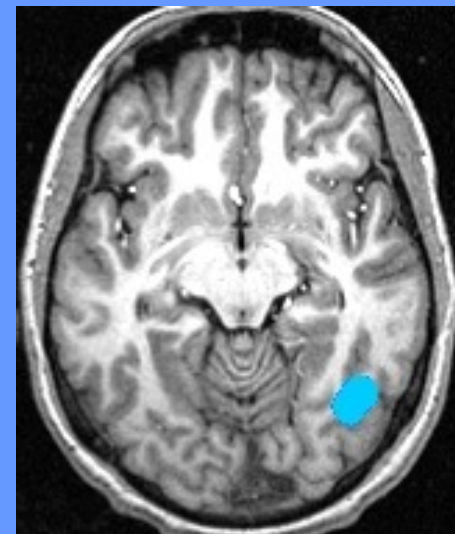
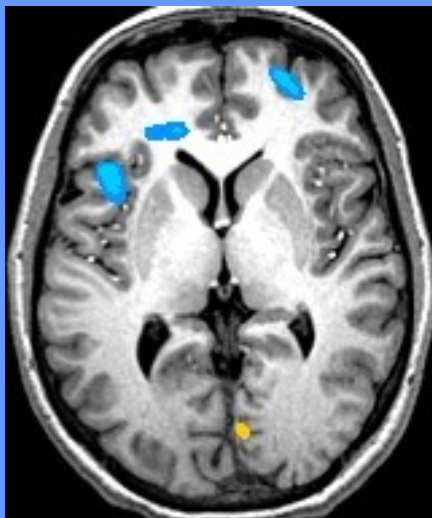
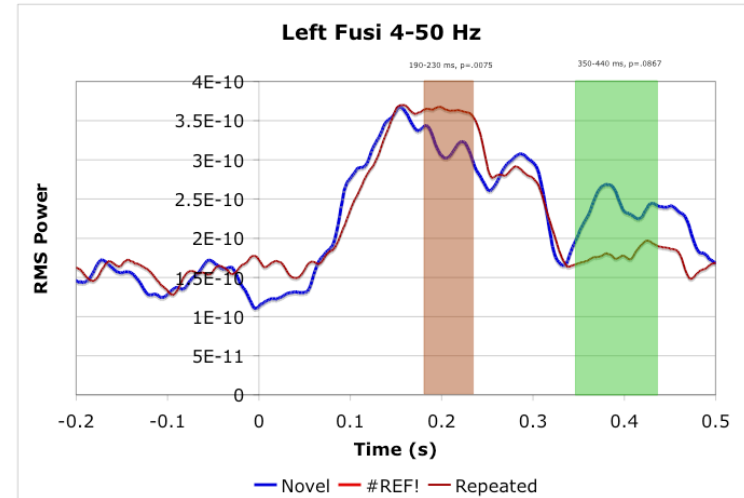
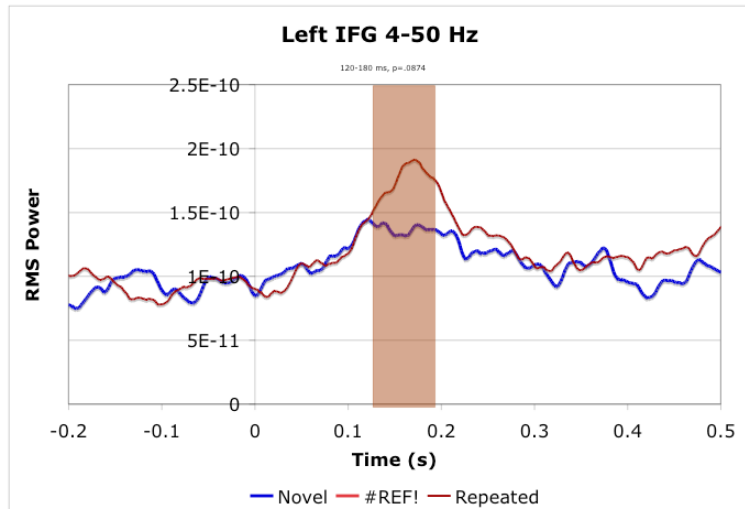


FIGURE 2: ROI templates drawn on a representative participant's MRI scan along with the average time courses from each of the left hemisphere ROIs. a: anticipatory period; e: encoding period; d: delay; r: response period.

Prefrontal Cortex Modulation during Anticipation of Working Memory Demands as Revealed by Magnetoencephalography

Mario Altamura,^{1,2} Terry E. Goldberg,¹ Brita Elvevåg,¹ Tom Holroyd,³ Frederick W. Carver,³ Daniel R. Weinberger,¹ and Richard Coppola^{1,3}

Top-down modulation during object priming (Gilbert et al)

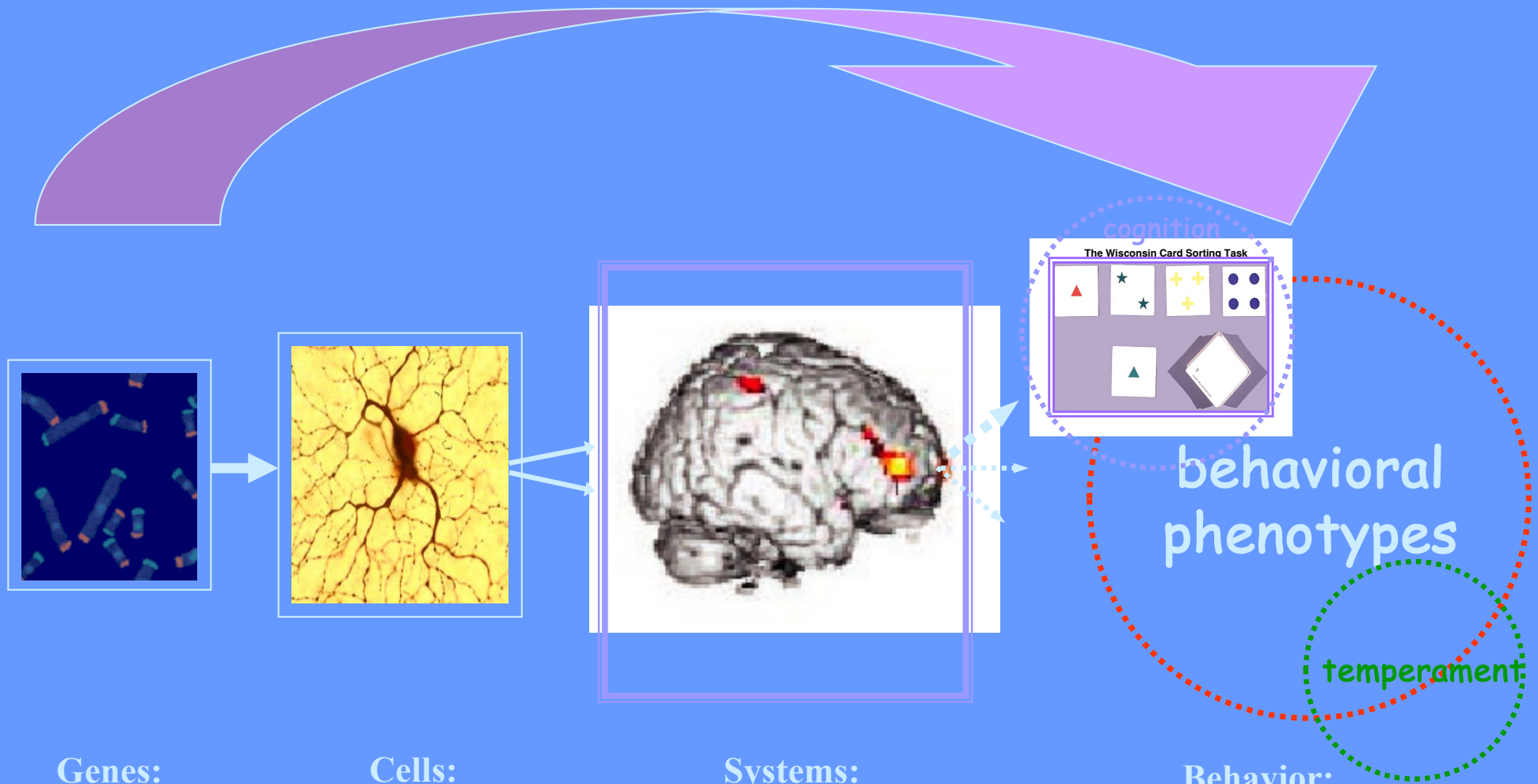


NIMH Sibling Study

Working Hypotheses:

- Different domains of cognitive impairment are heritable
- Define impairment on the basis of cognition, not diagnosis
- Schizophrenia qua schizophrenia is not inherited; impaired information processing is inherited and schizophrenia is emergent
- Investigate cognition via the n-back working memory task: compare probands, unaffected siblings, and normal controls

The path from here to there...



Genes:

*multiple
susceptibility
alleles each of
small effect*

Cells:

*subtle
molecular
abnormalities*

Systems:

*abnormal
information
processing*

Behavior:

*complex functional
interactions and
emergent
phenomena*

temperament

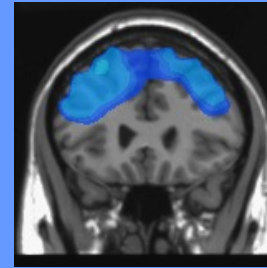
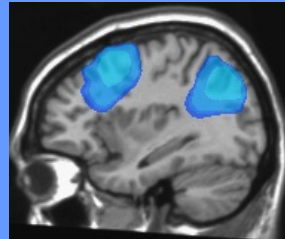
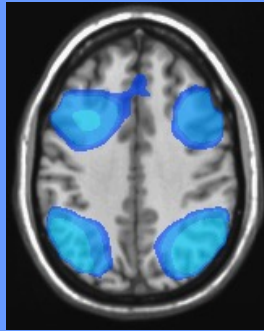
Group Means, 2-back vs. 0-back

Axial

Sagittal

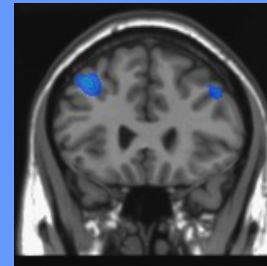
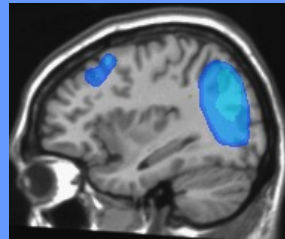
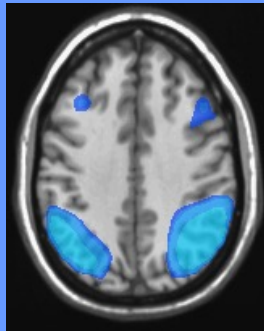
Coronal

NC
Mean



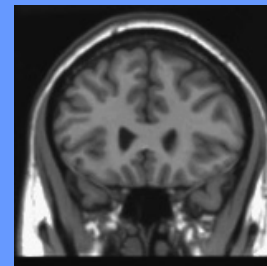
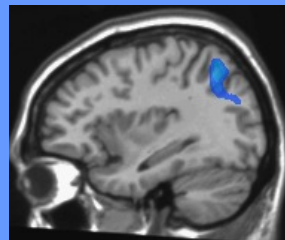
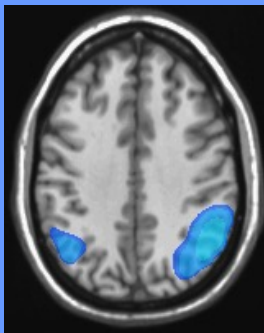
$p \leq .001, amp \geq .5$

Unaffected
Mean



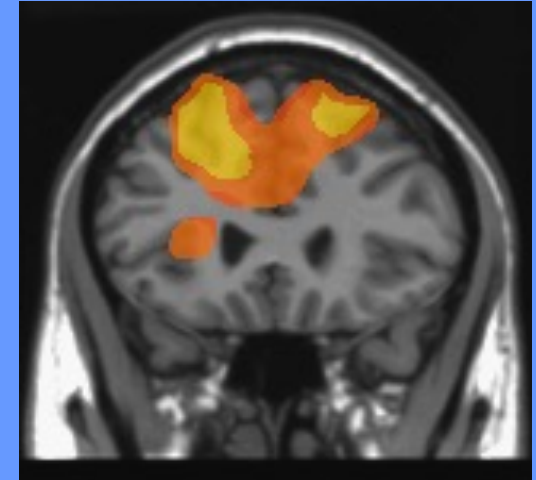
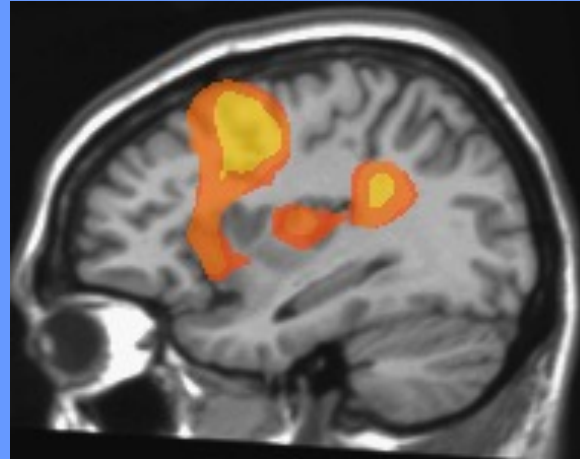
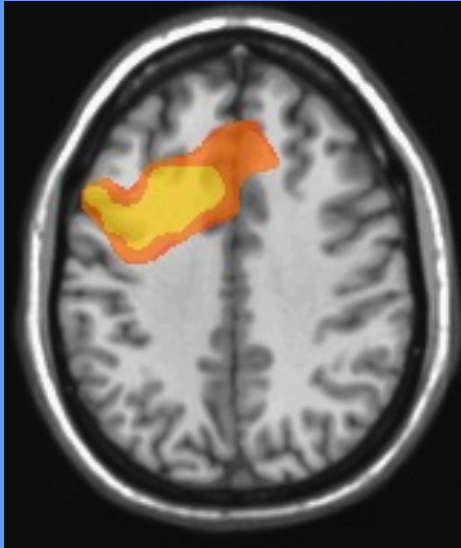
$p \leq .001, amp \geq .5$

Proband
Mean



$p \leq .001, amp \geq .5$

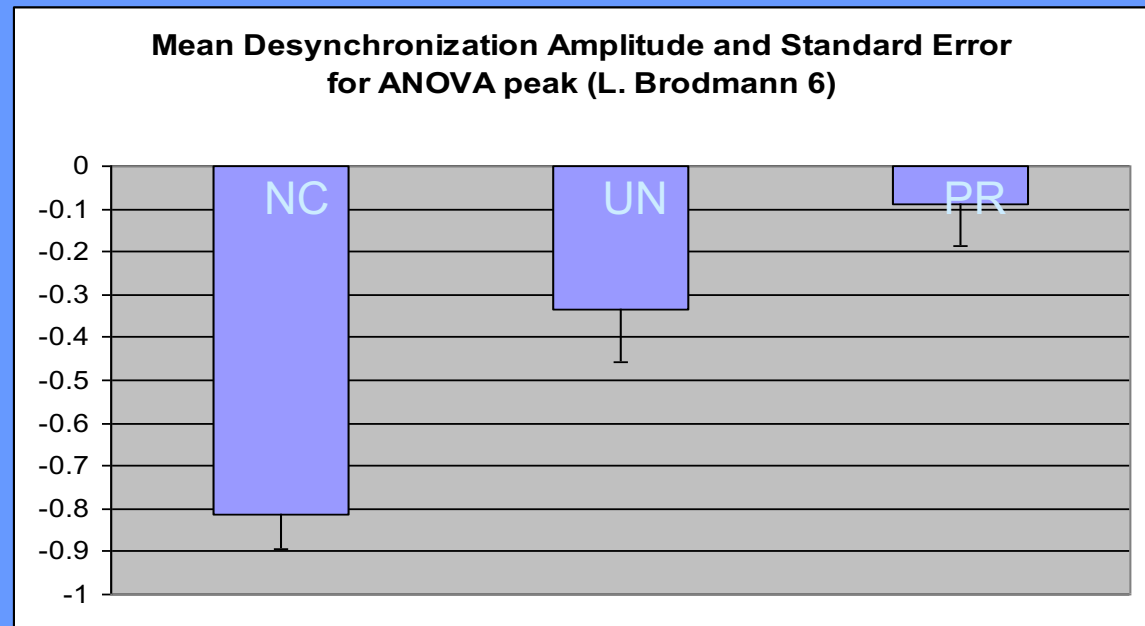
ANOVA, 2-back vs. 0-back



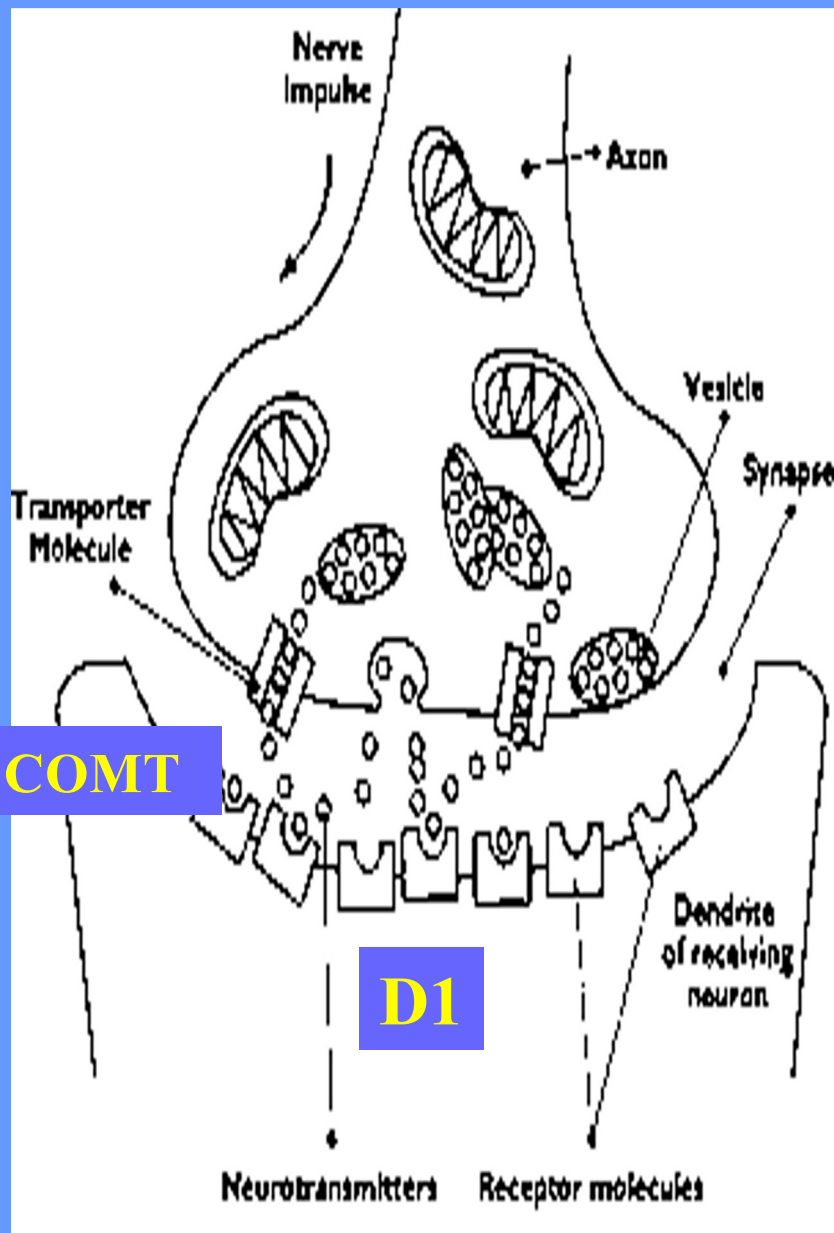
$p \leq .01$

ANOVA Peak Amplitudes

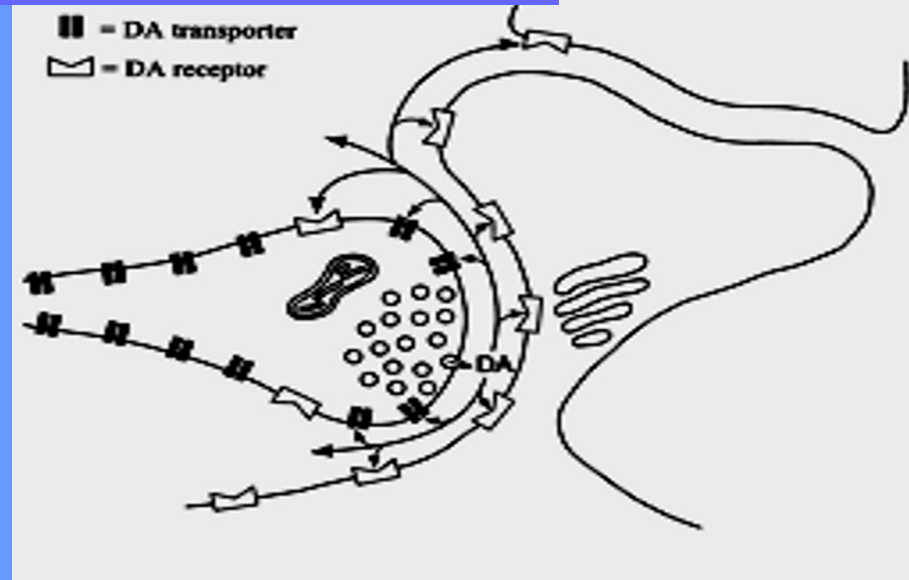
NC: sd = .959587
amp = -.815649
UN: sd = .994324
amp = -.334542
PR: sd = .920169
amp = -.087885



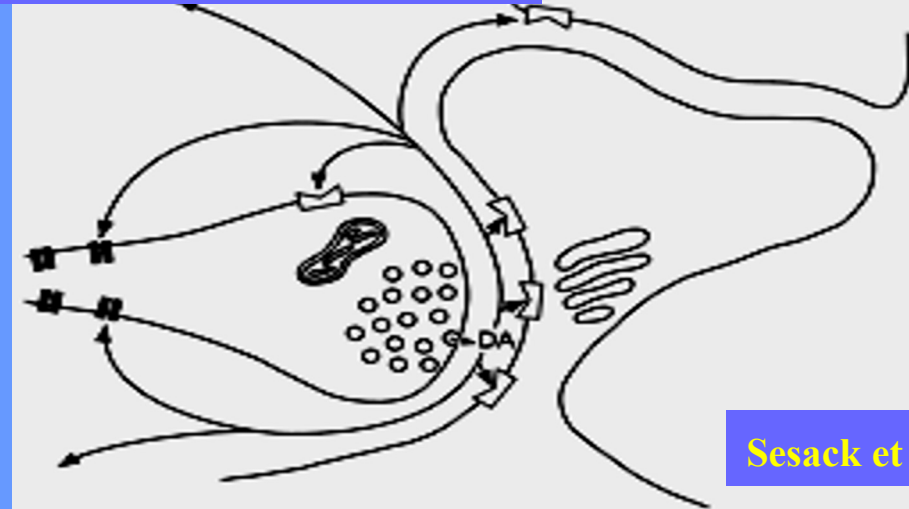
Candidate genes for working memory



Dorsolateral striatum

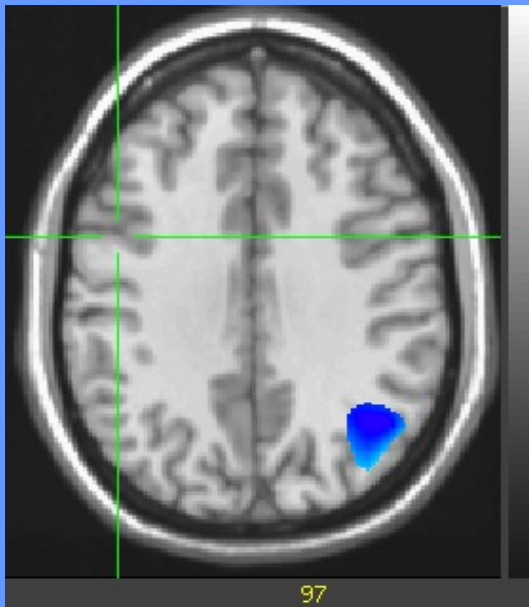


Prelimbic Cortex

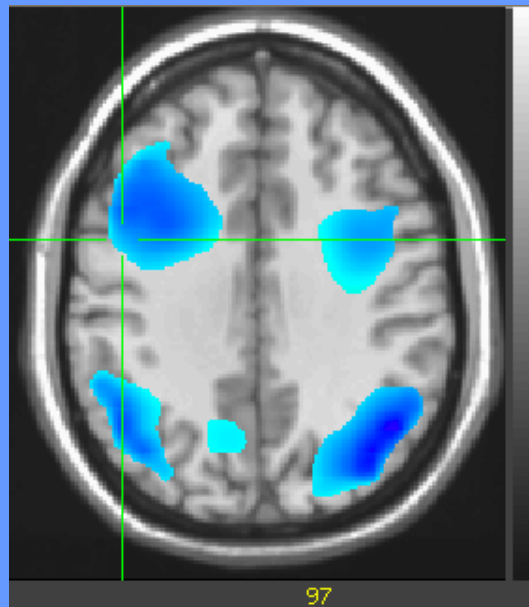


Sesack et al. 1998

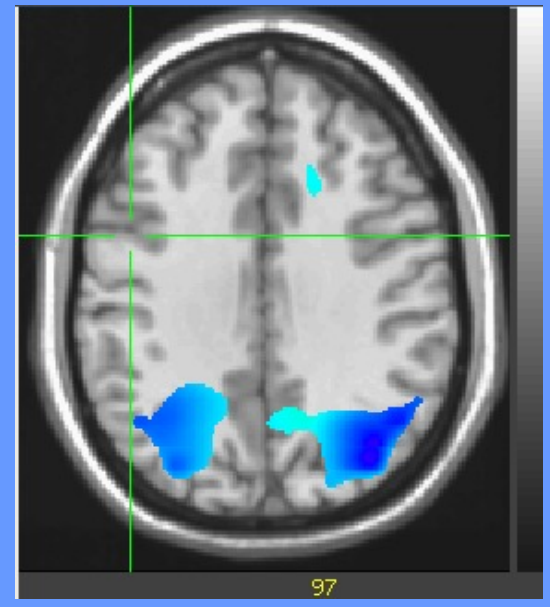
Group means 2-back activation $p < .001$
beta band, NC's n=66



valval



valmet



metmet

Left Rodmann 9 significant at $p < .05$ for genotype

Modulation of task-related MEG activity by SCN2A sodium channel genotype

A.H. Gerlich¹, F.W. Carver¹, T. Holroyd¹, J.H. Callicott², D. Dickinson², K.F. Berman², R. Coppola¹

¹MEG Core Facility, National Institute of Mental Health, Bethesda, MD, USA

²Clinical and Translational Neuroscience Branch, National Institute of Mental Health, Bethesda, MD, USA

Background

SCN2A, a gene that encodes the alpha-2 subunit of the voltage-gated type II sodium channel, mediates the conformational changes necessary for the formation of action potentials in the CNS. Past studies support that variants in SCN2A underlie certain epileptic seizures and impaired cognitive performance found in various developmental, intellectual, and social spectrum disorders. Additionally, there exists a disparity in general cognitive ability or "g" between carriers of the T allele (T/T or C/T) and those of the homozygous C allele (C/C), and this disparity differs in healthy controls from those with schizophrenia and their unaffected first-degree siblings. In Scult et al. (2015), correlation between fMRI activation in the dl-PFC and dACC was shown to significantly mediate cognitive ability with these disparities in healthy controls. Here, this investigation of genetic modulation is continued using magnetoencephalography.

Methods

Image Acquisition: MEG signals were recorded in a magnetically shielded room using a 275-channel whole head system (CTF). For each participant a structural MRI was co-registered with their MEG head coordinate system.

Task: The task was designed to assess working memory. The stimulus consisted of a diamond-shaped grid containing the digits 1 through 4. Using an inter-stimulus interval of 1.8 seconds, one of the four numbers appeared for 160 ms. Subjects were asked to respond to the appropriate previously-presented digit, as dictated by the specific task (0 Back, 1 Back, or 2 Back).



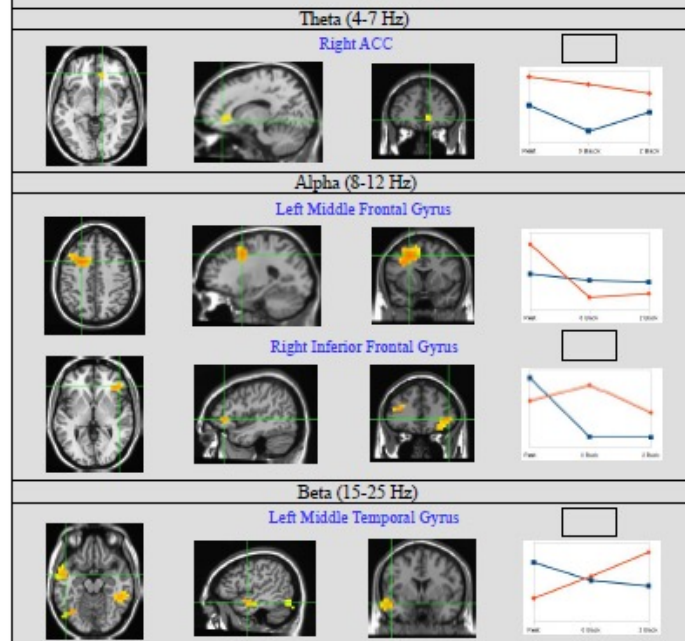
Genotype Acquisition: SCN2A SNP data was obtained from the NIMH Sibling Study. 30 carriers of the T allele (15 homozygous and 15 heterozygous) and 30 of the homozygous C allele were used.

Analysis: Synthetic aperture magnetometry (SAM) was used to estimate the sources of neuromagnetic activation. SAM creates an optimal spatial filter from MEG channel covariance to estimate source power in a specified time window and frequency band. Independent power estimates for the 2-back, 0-back, and Rest were performed at 5mm cubic voxels throughout the brain volume. The frequency bands were chosen from MEG channel power spectra, and the time windows were from 3s to 21s in each block with dummy blocks used for the resting recording. Each image was normalized by a noise estimate based on the signal covariance, and then converted to a Z-score. AFNI was used to align datasets into a common coordinate system and to perform statistics. A 2x3 genotype-by-task ANOVA was performed using 30 subjects for each genotype.

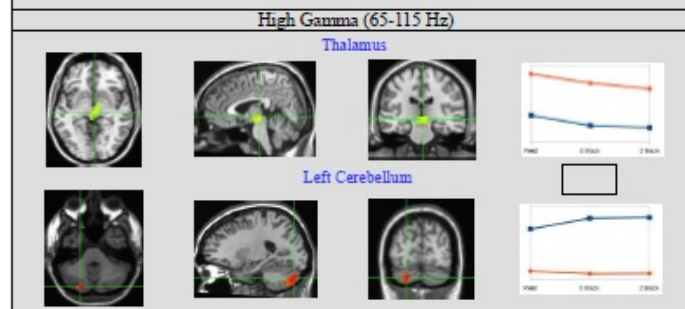
Results

At $p < 0.01$, the analysis revealed four cortical areas of interest as well as two sub-cortical regions. The theta band (4-7 Hz) showed a significant main effect between genotypes in the right ACC (TC/TT > CC). The alpha band (8-12 Hz) showed two significant interactions, one in the left middle frontal gyrus and the other in the right inferior frontal gyrus. The beta band (15-25 Hz) showed a significant interaction in the left middle temporal gyrus. The sub-cortical findings revealed a significant main effect in the high gamma band (65-115 Hz) in the region of the thalamus (TC/TT > CC) as well as in the left cerebellum (CC > TC/TT). At $p < 0.001$ and $q < 0.05$, there were two significant cortical interactions in the high gamma band, one in the dl-PFC and the other in the dACC and the medial frontal gyrus.

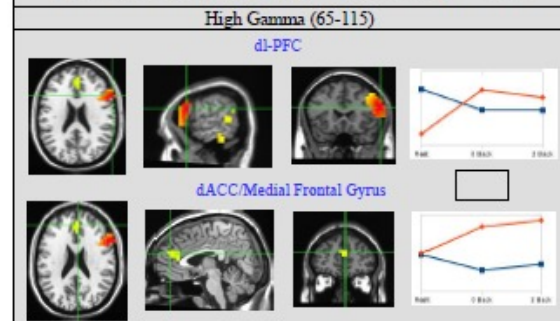
Cortical Findings at $p < 0.01$



Sub-cortical Findings at $p < 0.01$



Cortical Findings at $p < 0.001, q < 0.05$



Discussion

As in Scult et al. (2015), we found genotype-related activation differences in both the dl-PFC and the dACC (in which interactions were found in the high gamma band). Additional areas were also discovered, including regions of the temporal gyrus, inferior frontal gyrus, thalamus, and cerebellum.

Analysis of the alpha band revealed two interactions of genotype and task. The left medial frontal gyrus showed higher power for the TC/TT genotype during rest, but higher power for the CC genotype during both 0 Back and 2 Back. Interestingly, the right inferior frontal gyrus showed the opposite interaction, in which there was higher power for the CC genotype during rest, but higher power for the TC/TT genotype during both the 0 back and 2 Back.

Regarding the sub-cortical regions (thalamus and cerebellum), it is interesting that (while both exhibited main effects) the thalamus showed higher power across all tasks for the TC/TT genotype, while the cerebellum showed higher power across all tasks for the CC genotype.

The only frequency with significant results at $q < 0.05$ was the gamma band (65-115 Hz), suggesting that definitive differences may exist between genotypes at higher frequencies. As high gamma is a relatively new area of investigation, more studies are necessary to parse out the meaning of these results.

The effects of genotype on activation patterns found here may be implicated in differences in cognitive processing and/or intellectual functioning in healthy controls, as mediated by the conformational differences in the type II sodium channel. Further studies utilizing these (as well as other) imaging techniques may also support similar findings in affected populations (e.g. schizophrenia, spectrum, and neurodevelopmental disorders).

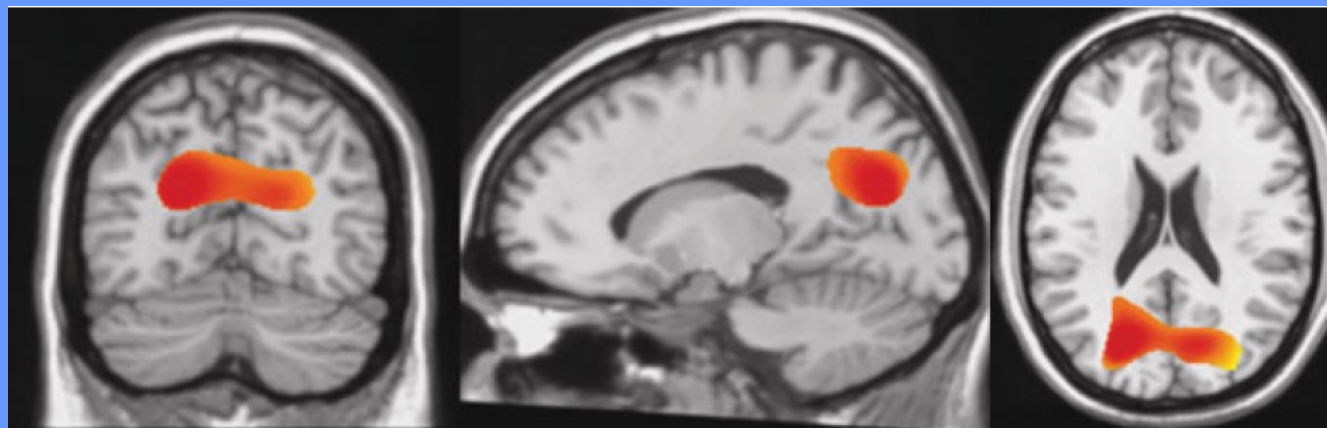
References

- Dickinson, D., Straub, R. E., Trampush, J. W., Gao, Y., Feng, N., Xie, B., ... Weinberger, D. R. (2014). Differential effects of common variants in SCN2A on general cognitive ability, brain physiology, and messenger RNA expression in schizophrenia cases and control individuals. *JAMA Psychiatry*, 71(6), 647-656. Retrieved from <http://archpsyc.jamanetwork.com/>
- Scult, M., Trampush, J. W., Zheng, F., Corley, E. D., Lencz, T., Malhotra, A. K., ... Hariri, A. R. (2015). A common polymorphism in SCN2A predicts general cognitive ability through effects on pFC physiology. *Journal of Cognitive Neuroscience*, 27(9), 1766-74. doi:10.1162/jocn.2015.00826

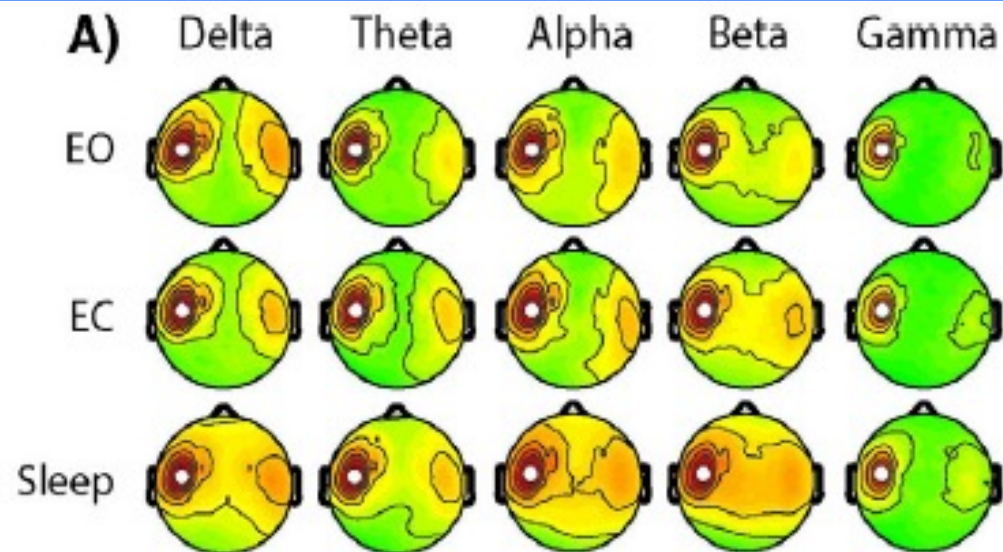
◆ Human Brain Mapping 30:3254–3264 (2009) ◆

Magnetoencephalographic Gamma Power Reduction in Patients with Schizophrenia During Resting Condition

Lindsay Rutter,¹ Frederick W. Carver,¹ Tom Holroyd,¹
Sreenivasan Rajamoni Nadar,¹ Judy Mitchell-Francis,¹ Jose Apud,²
Daniel R. Weinberger,² and Richard Coppola^{1,2*}



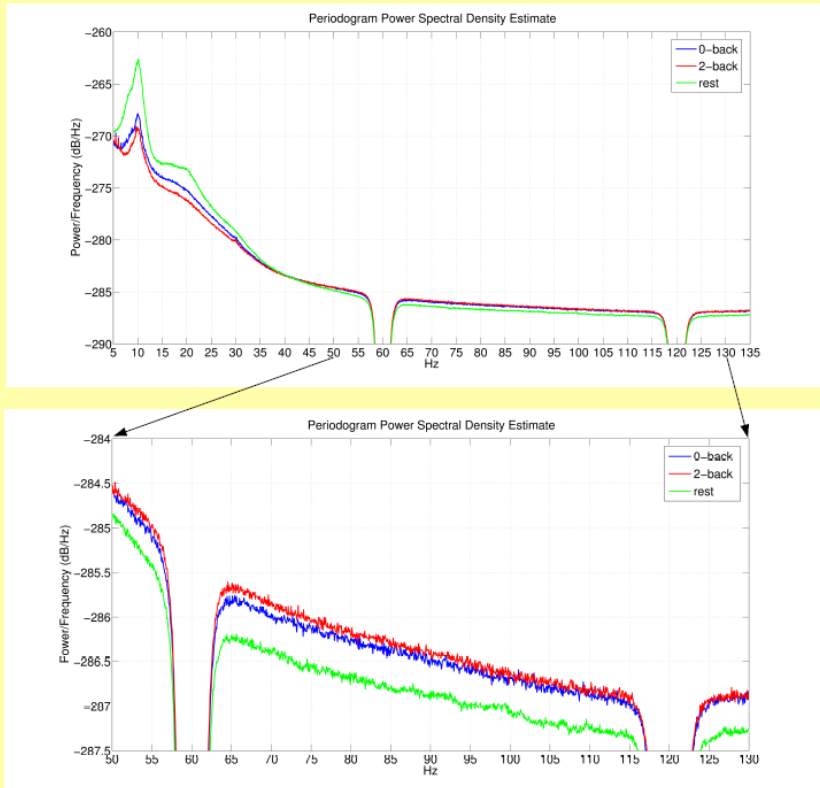
NeuroImage 51 (2010) 102–111



Large-scale spontaneous fluctuations and correlations in brain electrical activity observed with magnetoencephalography

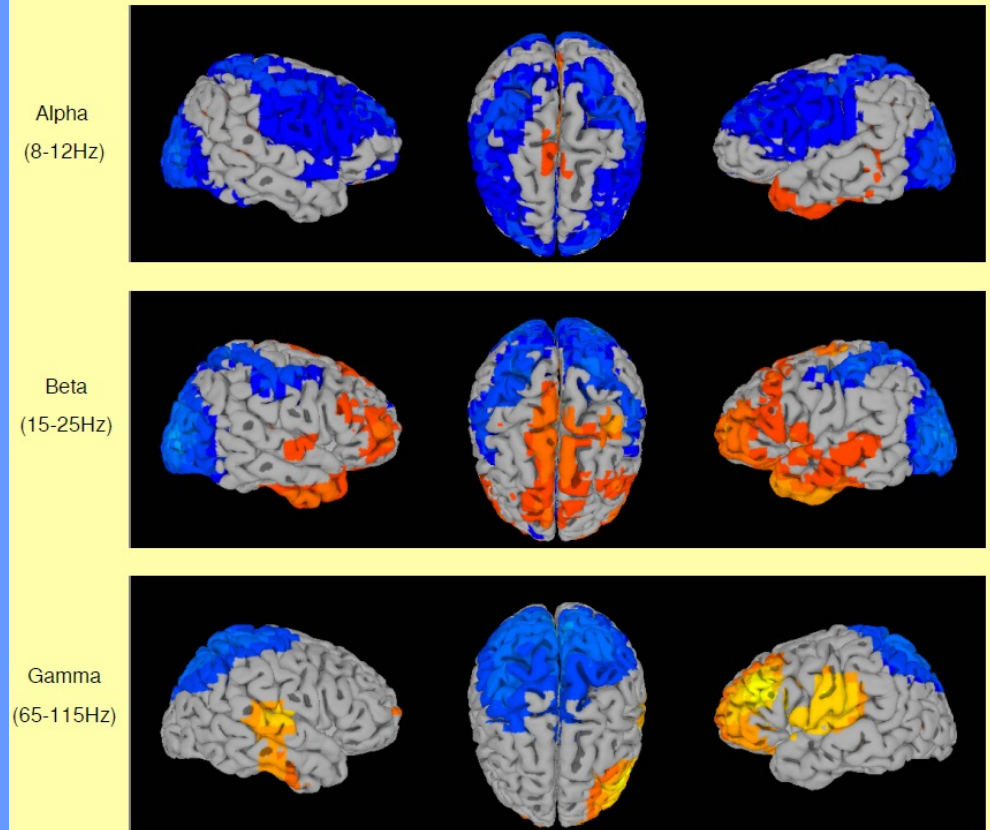
Zhongming Liu *, Masaki Fukunaga, Jacco A. de Zwart, Jeff H. Duyn

Power Spectra Comparing 2-back and 0-back to Rest



Mean spectra for all MEG channels comparing n-back blocks to dummy blocks in a separate resting eyes closed recording. Alpha and beta band desynchronization occurs in the N-back conditions relative to rest, with more desynchronization in the 2-back condition than the 0-back. The second chart zooms in to show broad band differences in high gamma power, including greater power in the 2-back relative to 0-back and rest.

MEG SAM 0-back > Rest



Contrast of 0-back and rest showing difference in signal power in frequency bands determined from the power spectra graphs above. Blue indicates less activation (desynchronization) in the 0-back, and red/yellow greater activation compared to rest ($p < .001$, $q < .05$). The contrast of 2-back to rest produced similar activation maps (results not shown).

Frequency-band specific changes in cortical MEG activation during a working memory task Carver et al SFN 2014

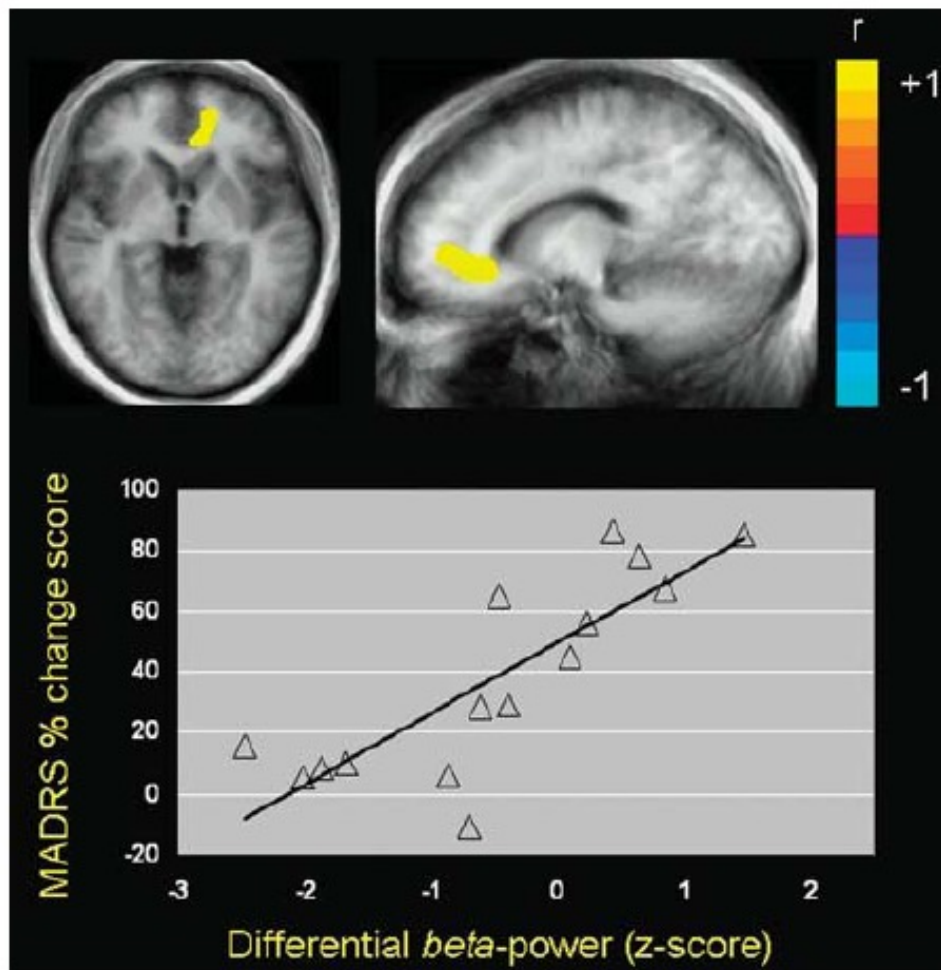


Figure 1 Pearson correlation between beta desynchronization in the anterior cingulate cortex (ACC) and change in depressive symptoms 230 min after ketamine infusion for the 2-back vs 1-back comparison in patients with MDD (ACC peak $x = -15$, $y = 45$, $z = -1$ mm; coordinates expressed according to the stereotaxic atlas of Talairach and Tournoux (Talairach and Tournoux, 1988)). These coordinates localize to the pregenual portion of the ACC, although the cluster of voxel t -values

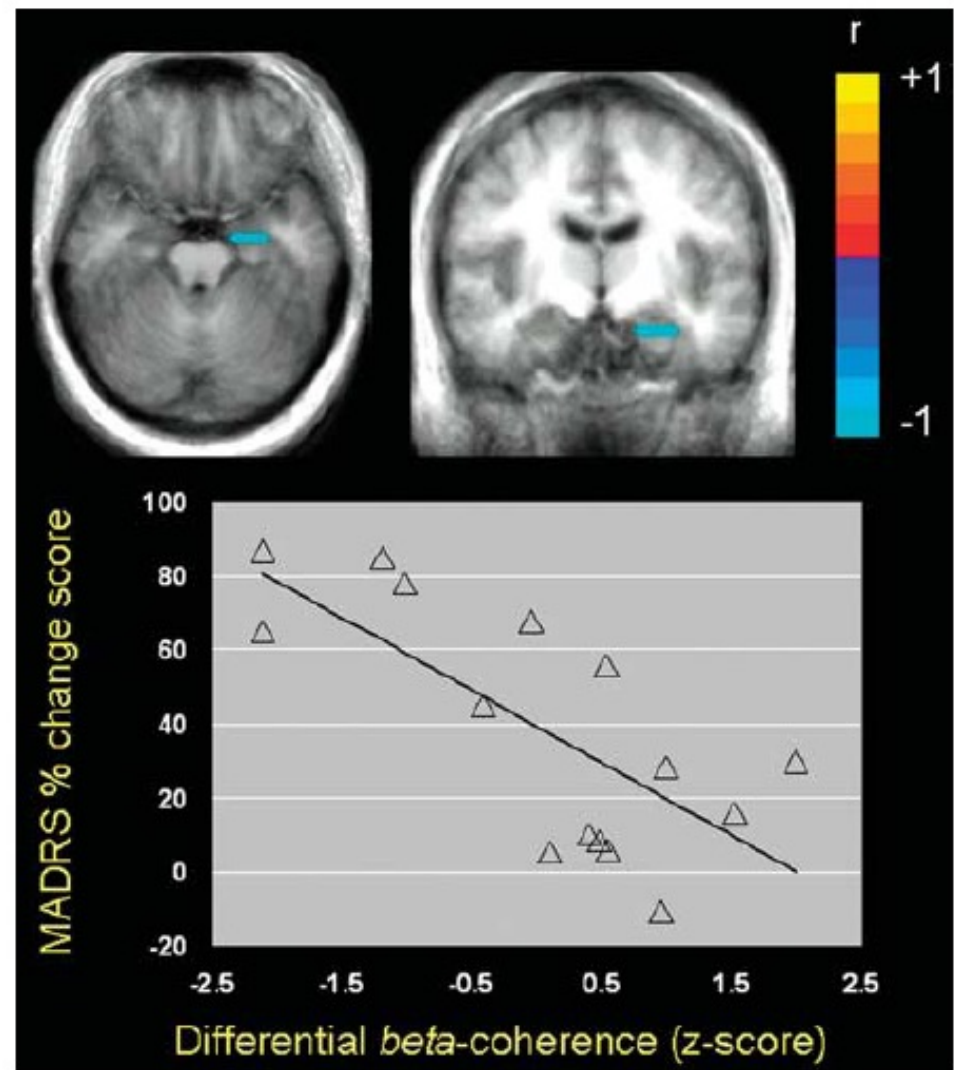
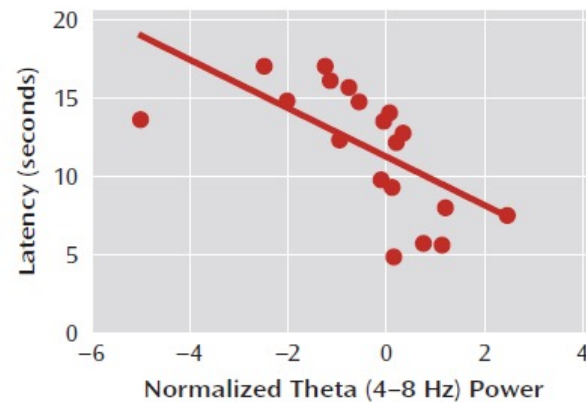
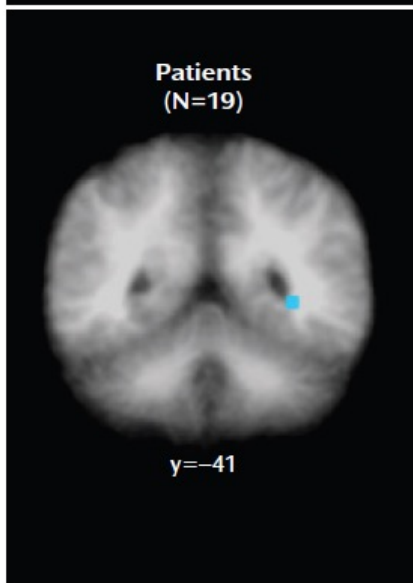
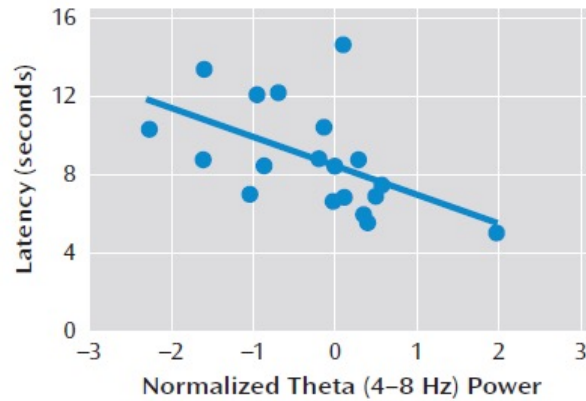
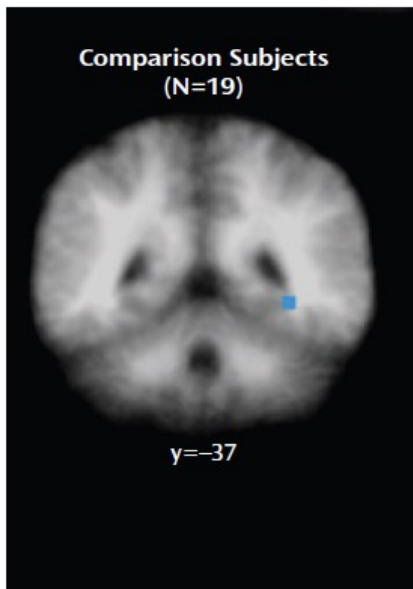


Figure 2 Pearson correlation between differential source coherence of the pgACC with the left amygdala and change in depressive symptoms 230 min after ketamine infusion for the 2-back vs 1-back comparison in patients with MDD (left amygdala peak: $x = -30$, $y = -7$, $z = -16$ mm; coordinates expressed according to the stereotaxic atlas of Talairach and Tournoux (Talairach and Tournoux, 1988)).

Anterior Cingulate Desynchronization and Functional Connectivity with the Amygdala During a Working Memory Task Predict Rapid Antidepressant Response to Ketamine

Neuropsychopharmacology (2010), 1–8

Giacomo Salvatore^{*1,2}, Brian R Cornwell², Fabio Sambataro³, David Latov^{1,2}, Veronica Colon-Rosario¹, Frederick Carver⁴, Tom Holroyd⁴, Nancy Diaz-Granados^{1,2}, Rodrigo Machado-Vieira^{1,2}, Christian Grillon², Wayne C Drevets² and Carlos A Zarate, Jr^{1,2}



Am J Psychiatry. 2010 Jul;167(7):836-44. Epub 2010 May 3.

Abnormal hippocampal functioning and impaired spatial navigation in depressed individuals: evidence from whole-head magnetoencephalography.

Cornwell BR, Salvatore G, Colon-Rosario V, Latov DR, Holroyd T, Carver FW, Coppola R, Manji HK, Zarate CA Jr, Grillon C.

Mood and Anxiety Disorders Program, NIMH, 15K North Dr., MSC 2670, Bethesda, MD 20892, USA. cornwellb@mail.nih.gov

Commentary

Psychiatric Stress Testing: Novel Strategy for Translational Psychopharmacology

Stephen M Stahl*^{1,2}

¹Department of Psychiatry, University of California, Carlsbad, CA, USA; ²Department of Psychiatry, University of Cambridge, Cambridge, UK

Neuropsychopharmacology (2010) 35, 1413–1414; doi:10.1038/npp.2010.29

A major focus of clinical neuroscience research today is to elucidate how reactions of brain circuits to stressful loads are regulated by genes and by psychiatric disorders. The study of Salvadore *et al* (2010) provides a glimpse into how such ‘psychiatric stress tests’ may also translate into predictors of who will respond to a specific drug.

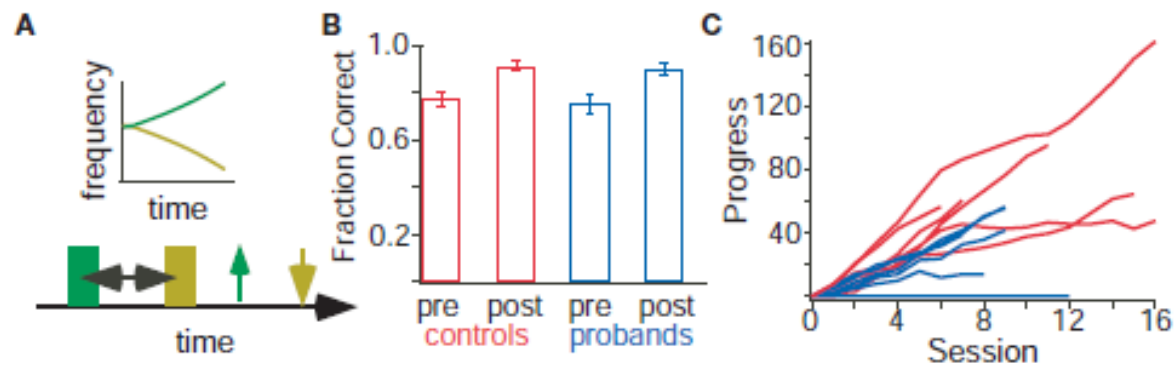


FIGURE 2 | Practice improves performance in the two-tone discrimination task. (A) In the task, two frequency modulated tones (green and yellow) are presented after a variable inter-stimulus interval. The subject makes two selections (up and down arrows) depending on the perceived direction of pitch modulation. **(B)** Progress in “high or low” pitch discrimination task during

practice sessions. For both control (red) and proband (blue) subjects, task difficulty during each 15 min session was adaptively adjusted to match skill level. Progress bars are proportional to the number of correct responses during the session and inversely proportional to the number of incorrect responses. **(C)** Task accuracy in controls (red) and probands (blue) before and after practice.



Functional brain network characterization and adaptivity during task practice in healthy volunteers and people with schizophrenia¹

Shennan Aibel Weiss^{1*}, Danielle S. Bassett², Daniel Rubinstein³, Tom Holroyd³, Jose Apud⁴, Dwight Dickinson⁴ and Richard Coppola⁴

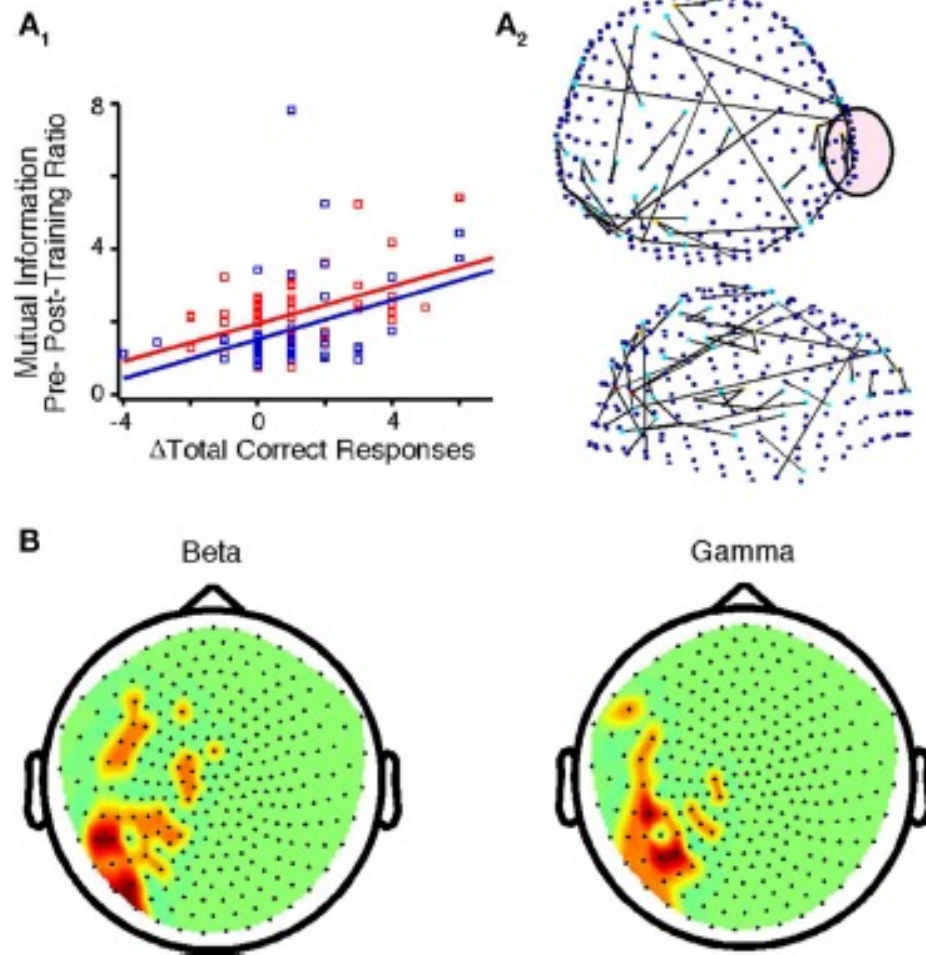


FIGURE 5 | Changes in functional brain networks after practice for controls and probands. (A₁) Correlations between Δ accuracy and Δ MI for controls ($F = 17.34$, $p < 1.0E-4$) and probands ($F = 21.15$, $p < 2.75E-5$) in the encircled sensor in (A₂). (A₂) Top and side view of sensors that exhibited the above correlation for all subjects in the beta band (FDR $p < 7.0E-5$). (B) Nodes in which Δ accuracy correlated positively with Δ power for all subjects in the beta and gamma frequency bands ($p < 0.0037$).

Midbrain dopamine differentially predicts neural response to happy and fearful facial expressions: ¹⁸FDOPA PET, fMRI, and MEG Findings



Tiffany A. Nash^{1,2}, Mbemba Jabbi^{1,2}, Philip Kohn^{1,2}, Angela Ianni^{1,2}, Tom Holroyd³, Frederick Carver³,
Shane Kippenhan¹, Richard Coppola, and Karen Faith Berman^{1,2}



INTRODUCTION

The midbrain ventral tegmental area and substantia nigra are the main source of striatal and mesolimbic dopamine (DA). Though it is well-documented that DA is involved in motivational signaling¹, the specific role of midbrain DA in modulating human brain response to emotions remains largely unknown. Because DA differentially codes positive vs. negative signals in a time-dependent fashion^{2,3}, we accounted for the dynamics aspect of facial emotional stimuli in the present experiment, as they evolve into full blown emotional expressions over time. In line with the excitation or depression of DA neurons in response to rewarding and aversive stimuli³, respectively, we predicted dissociable influences of midbrain DA synthesis on neural responses to emotional dynamics for positive vs. aversive social stimuli. Further, we anticipated that these influences would be observed in regions innervated by midbrain DA (Figure 1).

To test these hypotheses, we investigated the relationship between midbrain DA synthesis, measured with ¹⁸FDOPA PET, and BOLD response to specific stimulus attributes (duration and dynamics) of happy and fearful facial expressions. In order to better capture the temporal dynamics of DA-mediated neural response—a sub-second response—we examined the oscillatory response to the stimuli using magnetoencephalography (MEG). We particularly focused on gamma band oscillations, which have been associated with emotional processing⁴, and which have been found to be modulated by DA agonists⁵.

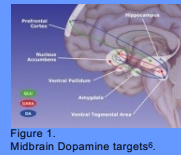


Figure 1. Midbrain Dopamine targets⁶.

METHODS

functional magnetic resonance imaging (fMRI)

- Twenty-one participants (6 females; mean age= 31.19) viewed short (1s) and long (3s) presentations of dynamic and static emotional (fear and happiness) or neutral (for dynamic stimuli, eye blinks) facial expressions (Figure 2).
- Data acquired on 3T; TR = 2.21s, TE = 75, number of slices = 27, FOV = 20
- Preprocessing and first level analyses of the fMRI response to emotions were carried out using SPM5.



Figure 2. Sample frame of videos. The static pictures used are shown in fourth frame.

Magnetoencephalography (MEG)

- Data acquired for 16 of the 21 participants (4 females; mean age=34.2).
- CTF 275 MEG system with a whole-head array of 275 radial 1st order gradiometer/SQUID channels⁷.
- Coregistration of subjects' MEG scans to their anatomical MRIs (Figure 3).
- Synthetic aperture magnetometry, a method for estimation of source power for each voxel of the brain using a beamformer, was carried out.



Figure 3. Coregistration of MEG and MRI

Positron emission tomography (PET)

- Two sixty-second, 12 mCi [¹⁸O]H₂O rCBF emission scans, and a 90-minute series of dynamic 16 mCi ¹⁸F-DOPA emission scans were acquired following oral administration of carbidopa to decrease peripheral metabolism.
- Using a voxel-wise Patlak method with a cerebellum reference region, FDOPA Ki, reflecting presynaptic DA synthesis, was determined for every voxel in the brain.
- A midbrain volume of interest was manually delineated on each individual's structural MRI (Figure 4) and coregistered to the native space FDOPA PET scans for extraction of average midbrain Ki values.



Figure 4. Example MB mask.

• Correlation analyses were performed using midbrain Ki values as predictors of BOLD response and MEG signal response in the gamma frequency band (30-50Hz). Results are threshold at 0.005, uncorrected, for display. Significance is reported for peak voxels.

RESULTS

DA-Modulated Neural Response to Positive Stimuli

Dynamics

DA-BOLD Coupling During Viewing of Static Happiness

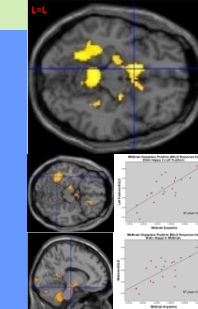


Figure 5. MB DA Correlates with BOLD in left fusiform ($p=2.2 \times 10^{-5}$) and midbrain ($p=0.001$)

DA-Gamma Coupling During Viewing of Static Happiness

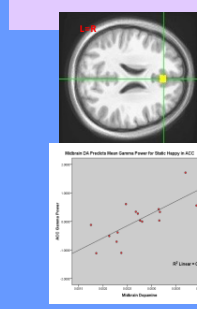


Figure 6. a) MB DA correlates with gamma power in ACC ($p=0.001$)

DA-BOLD Coupling During Viewing of Short Happiness

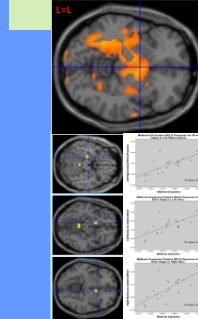


Figure 7. MB DA Correlates with BOLD in left hippocampus ($p=1.79 \times 10^{-4}$), left NAcc ($p=1.88 \times 10^{-4}$), right NAcc ($p=2.29 \times 10^{-4}$)

DA-Gamma Coupling During Viewing of Short Happiness

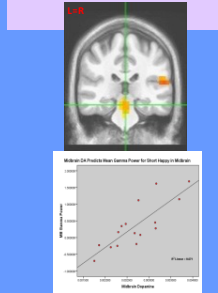


Figure 8. a) MB DA correlates with gamma power in left STS and midbrain ($p=0.001$)

DA-Modulated Neural Response to Negative Stimuli

Dynamics

DA-BOLD Coupling During Viewing of Dynamic Fear

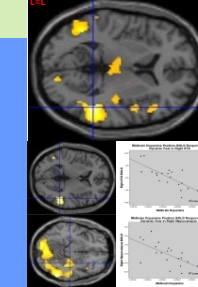


Figure 9. MB DA Correlates with BOLD in right STS ($p=1.8 \times 10^{-5}$) and right hippocampus ($p=0.001$)

DA-Gamma Coupling During Viewing of Dynamic Fear

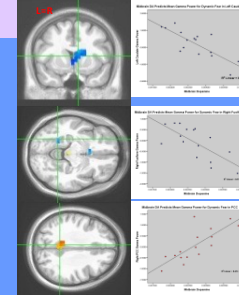


Figure 10. a) MB DA correlates with gamma power in left caudate ($p=0.001$), right NAcc ($p=0.001$), and right fusiform ($p=0.002$)

Duration

DA-Gamma Coupling During Viewing of Short Fear

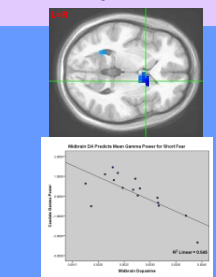


Figure 11. a) MB DA correlates with gamma power in left caudate ($p=0.001$)

DISCUSSION

DA differentially mediated neural response to environmentally-relevant stimulus attributes in a valence-specific fashion. While there was a largely positive DA-mediated neural response for happy expressions, negative relations were apparent between DA and neural response for fearful stimuli. These results suggest that happy and fearful facial expressions may provoke reward and aversion, respectively, and are in line with previous studies demonstrating an excitatory role of DA in response to reward and an inhibitory role in response to aversive stimuli.

Our results support previous research on the role of DA in reward coding and fear processing⁸, and confirm a role for DA in modulation of emotions. The DA modulated gamma oscillatory findings may reflect faster, more transient neural coding of emotional information, which may not have been captured by fMRI's coarser temporal resolution⁹. These differential findings for negative and positive emotions offer potential insight for studies of affective disorders.

REFERENCES: 1. Wise R Neurotox Res 2008. 2. Matsumoto M et al. Nature 2009. 3. Schultz W Annu Rev Neurosci 2007. 4. Luo Q Neuroimage 2007. 5. Brown et al J Neurosci 2001. 6. Ferrer et al. Drugs Fut 2007. 7. Fife A et al. Conf Biomagnetism 2002. 8. Wise R Nature Rev Neurosci 2004. 9. ...

Abnormalities in Resting State Connectivity in Bipolar Disorder

Allison C. Nugent¹, Stephen E. Robinson², Richard Coppola², Maura L. Furey¹, Carlos A. Zarate, Jr.¹

¹Experimental Therapeutics and Pathophysiology Branch, National Institute of Mental Health, National Institutes of Health, Bethesda MD, USA

²NIMH Magnetoencephalography Core Facility, National Institute of Mental Health, National Institutes of Health, Bethesda MD, USA

1. Background

- ICA analysis on band-pass limited Hilbert-envelope MEG resting state data reveals similar networks as those seen in fMRI (1).
- Regions within these networks exhibit correlated low frequency fluctuations of the smoothed Hilbert envelope.
- We previously demonstrated reduced connectivity in MDD compared to healthy subjects between a precentral/middle frontal C and subgenual anterior cingulate cortex (sgACC), as well as increased connectivity within limbic/temporal networks (2). This is the first similar analysis in bipolar disorder (BD).

2. Methods

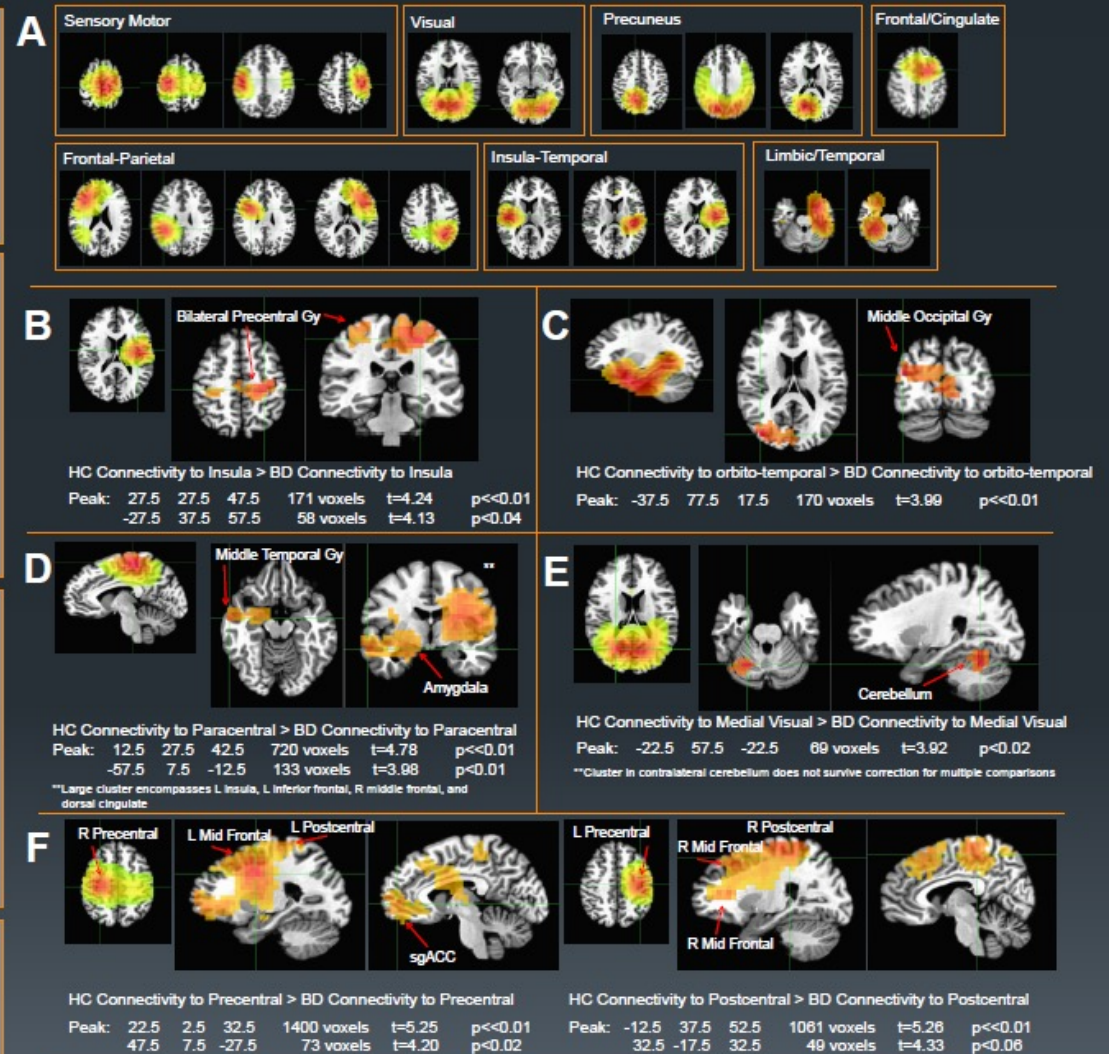
- MEG recordings were acquired for 17 subjects with BD (age=45±12.7, 7 female) and 16 control (HC) subjects (age=39±8.6, 8 female). Subjects did not differ significantly on age ($p>0.05$). Twelve BD subjects were medicated with either lithium or valproate monotherapy.
- MEG acquired on a 275-channel CTF system at 1200Hz for 260s, T1 MRI scans were acquired for coregistration.
- Recordings were beta (14-30 Hz) band-pass filtered, and projected into anatomical space of the T1 MRI at isotropic 5mm resolution using SAM (3)
- Hilbert envelopes were calculated, smoothed, and sampled at 1Hz
- Data from all subjects was temporally concatenated after transformation to standard space, and temporal ICA was performed to extract 25 independent components (ICs)
- Linear regression was used to obtain group and individual subject IC maps
- Subject maps were compared between groups using independent samples t-tests in AFNI (Analysis of Functional Images, NIMH/NIH Bethesda MD) (4)
- T-score images were initially thresholded at $p<0.005$ uncorrected and clusters surviving correction for multiple comparisons at $p_{\text{corr}}<0.05$ are reported.

3. Results

- Out of 25 estimated components, 20 were either distributed networks or single nodes.
- Connectivity between a left insular node and bilateral motor cortex was reduced in BD.
- Connectivity between a unique limbic network (encompassing orbitofrontal and parahippocampal cortex) and middle occipital cortex was reduced in BD.
- Connectivity between an IC covering bilateral paracentral motor areas with insula and amygdala was reduced in BD.
- Connectivity between a medial visual IC and cerebellum was reduced in BD.
- Connectivity between left and right lateralized sensorimotor IC's was reduced in BD to similar areas in contralateral postcentral gyrus, superior/middle frontal gyrus, and inferior frontal gyrus. Connectivity to R precentral gyrus was additionally reduced in the subgenual cingulate and orbitofrontal cortex, similar to our finding in subjects with MDD (2).

4. Discussion

- In this preliminary study of MEG resting state connectivity in bipolar disorder, the first to use an ICA analysis, we have found a widespread pattern of reduced connectivity compared to controls.
- Similar to healthy controls, we find reduced connectivity between a precentral motor network and subgenual ACC (2). In addition, our subjects with BD show decreased connectivity between motor regions and the insula and amygdala, regions known to interact with the sgACC.
- In general, BD subjects exhibited impaired connectivity to locations contralateral to the primary node location. This is consistent with reduced corpus callosum volume in BD (5) and impaired inter-hemispheric connectivity (6).
- MEG resting state connectivity may reveal unique abnormalities in BD, potentially informing treatment.



5. References

- Brookes, M.J., et al. (2011), PNAS 108(40): 16783-16788.
- Nugent, A.C., et al. (2014), Society for Neuroscience Annual Meeting, San Diego, CA.
- Robinson and Vrba (1999), In Recent Advances in Biomagnetism, pp. 302-305.
- AFNI: Analysis of Functional NeuroImages, @NIMH/NIH, Bethesda, MD, <http://afni.nimh.nih.gov>
- Amone, D., et al. (2008), Acta Psychiatrica Scandinavica 115(5):357-362.
- Leow, A., et al. (2013), Biological Psychiatry 72(2):183-193.

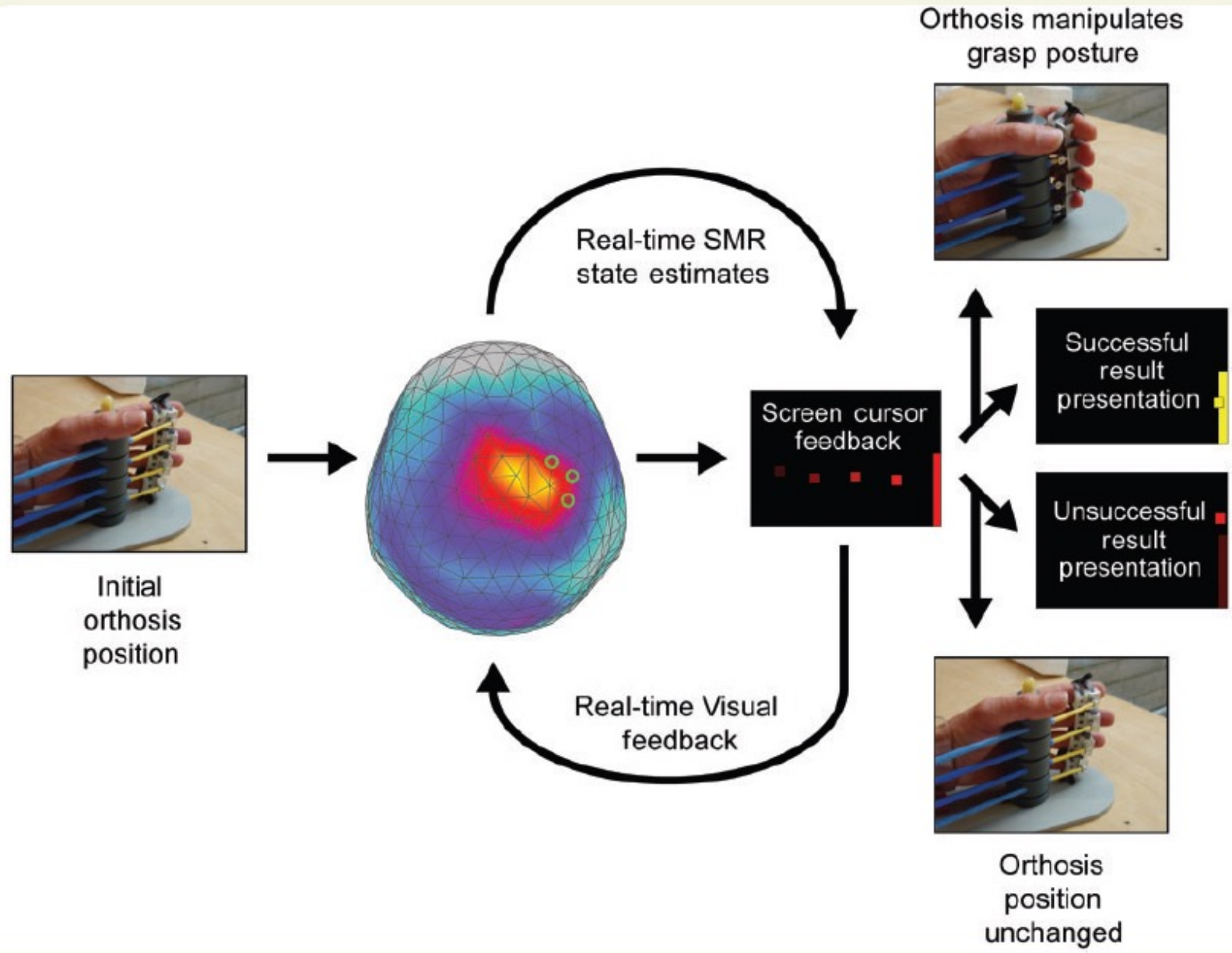
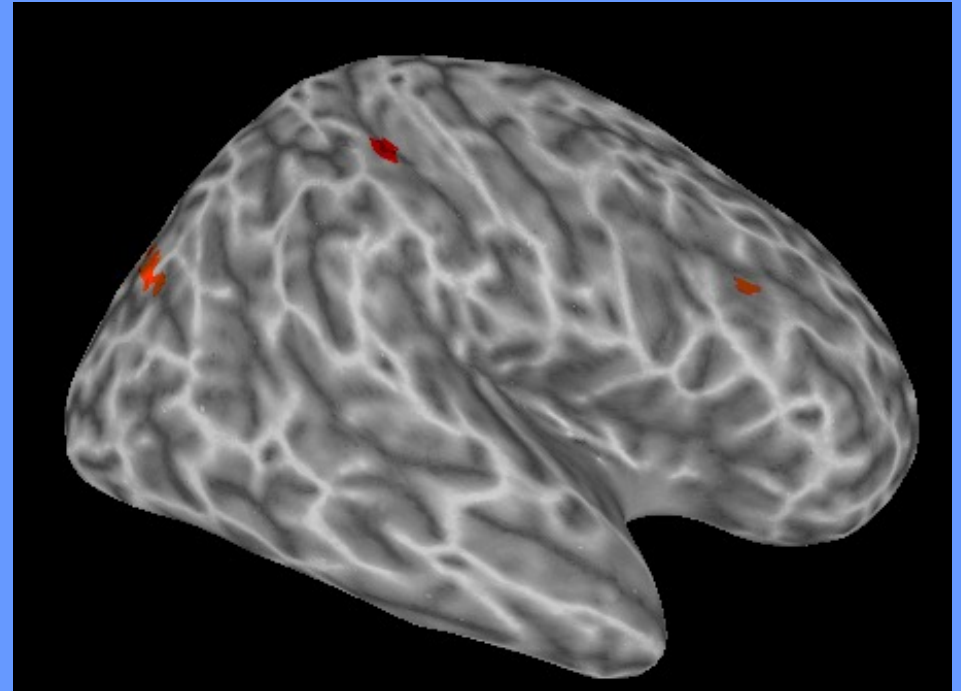
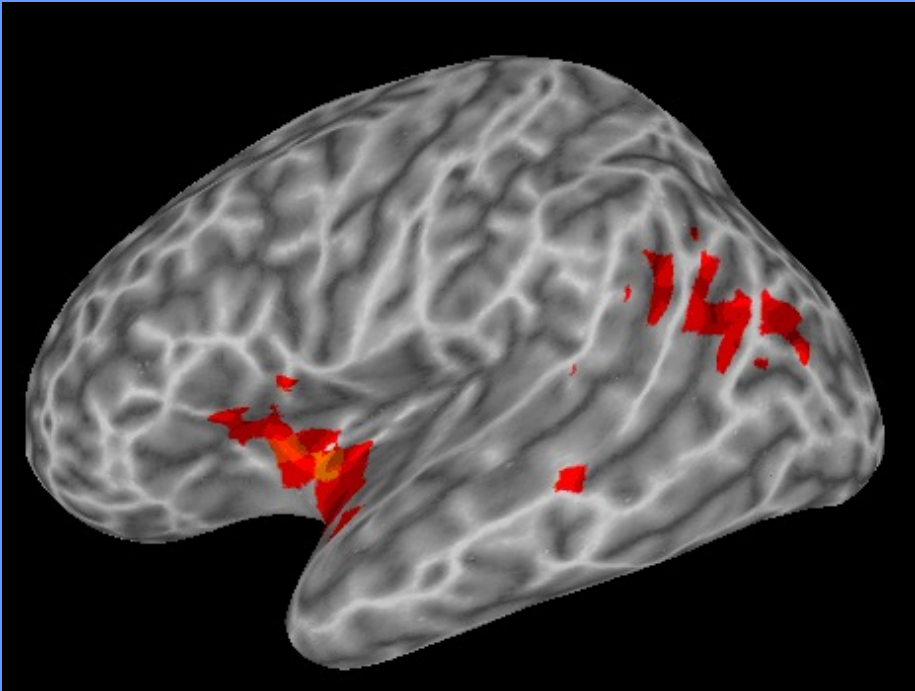


Figure 2 Trial description for sensorimotor rhythm (SMR) modulation through grasping imagery training. Whole-head magnetoence-

Gamma band activity during auditory stimulation



NIMH MEG Core Facility

- Dr. Richard Coppola, Director
- Dr. Tom Holroyd, Staff Scientist
- Dr. Fred Carver
- Dr. Stephan Robinson
- Judy Mitchell-Francis, Lab Mgr
- Samantha Fradkin, Post-Bac IRTA

CTNB Sib Study

- K. Berman
- J. Apud
- S. Marengo
- J.H. Callicott

MAP

- Carlos Zarate
- Alison Nugent
- Brian Cornwell



User Information

[MEG Setup](#)

[MEG Analysis](#)

[Schedule](#)

[User Meetings](#)

[Lab Status](#)

[Forms](#)

[Brochures](#)

[Manuals and Tutorials](#)

[Links](#)

User Information

Becoming a User

[Subject Guidelines](#)

Detailed Facility Description

[Task Programming](#)

[Training/Pilot](#)

[User Meetings](#)

[Quality Assurance](#)

Search



POLICIES AND PROCEDURES

These documents comprise the official policies and procedures for the MEG lab.

- [Mission Statement](#)
- **Operations (1.00)**
 - [Hours of Operation](#)
 - [Laboratory Access](#)
 - [Dress Code](#)
- **Scheduling (2.00)**
 - [Scheduling Procedures](#)
 - [Facility Access Requests](#)
- **User/Subject Guidelines (3.00)**
 - [User Guidelines](#)
 - [Normal Control / Subject Guidelines](#)
 - [Inpatient Guidelines](#)
 - [Data Access Accounts / Data Access](#)
 - [Variance Reporting](#)
- **MEG / EEG Setup (4.00)**
 - [MEG Setup Procedures](#)
 - [Fiducial Points Placement](#)
 - [EEG Easy Cap Setup Procedures](#)
 - [EEG 10-20 Electrode Placement System](#)
 - [Electrodes Specifications Guidelines](#)
 - [Polhemus Digitization System](#)
 - [Head Stabilization Pillow](#)
 - [MEG System Impedance Check](#)
 - [Grass Impedance Meter Check](#)
- **Magnetically Shielded Room (MSR) / Support System (5.00)**
 - [Magnetically Shielded Room \(MSR\)](#)
 - [Gantry Operation](#)
 - [Chair Operation](#)
 - [Bed Operation](#)
- **Stimulus / Response Equipment (6.00)**
 - [Panasonic DLP Projector](#)
 - [Grass Nerve / Muscle Stimulator](#)
 - [Auditory Stimulation](#)
 - [Response Pads](#)
 - [VCR Operation](#)
 - [Video Camera Operation](#)
 - [Voice Intercom System Operation](#)
- [Video Display Monitor](#)
- [Infrared Lighting](#)
- **Data Acquisition (7.00)**
 - [Data Acquisition](#)
 - [Transferring Data to the RAID Array](#)
- **Infection Control (9.00)**
 - [Infection Control](#)
 - [Cleaning, Disinfection & Sterilization of MEG Equipment](#)
 - [Hand Hygiene, Cleaning & Washing Procedures](#)
 - [Infection Control - CHS Processing Procedure](#)
- **Quality Assurance / Risk Management (10.00)**
 - [Quality Improvement Plan](#)
 - [MEG System Calibration](#)
 - [Routine Noise Collection](#)
 - [Head Coil Calibration Procedures](#)
 - [Magnetic Phantom Calibration](#)
 - [EEG System Calibration](#)
 - [MEG Lab System Monitors](#)
 - [Material Safety and Data Sheets \(MSD Sheets\)](#)
 - [Liquid Helium Safety](#)
 - [Compressed Helium Gas Safety](#)
 - [Compressed Helium Gas Level Check](#)
 - [Liquid Helium Refill Procedure](#)
 - [Possible Seizure Event](#)
 - [Medical Emergency / Suspected Cardiac or Respiratory Event](#)
 - [Laboratory Safety](#)
 - [Subject / Patient Identification](#)
 - [Power Failure](#)
 - [Chemical or Biological Materials Incident](#)
 - [Radiation Incident](#)
 - [Bomb Threat Incident](#)
 - [Evacuation / Emergency Preparedness Plan](#)
 - [Variance / Safety / QI Reporting](#)
- **Training & Education (11.00)**
 - [Training & Education](#)
- **Compliance / Credentialing (12.00)**
 - [Compliance/Credentialing](#)

NIMH MEG Core Facility Schedule

NIMH MEG Core Facility Wisdom of the Moment
 Time is infinite. In particular, you can schedule slots for evening times by clicking on any slot and changing the start time.

January 25, 2015 - January 31, 2015

(Week 03)

Administrator



	Sun January 25	Mon January 26	Tue January 27	Wed January 28	Thu January 29	Fri January 30
8:00					8:00> Grillon/Balderston	
8:30						
9:00				9:00> Zarate/Berg		
9:30		9:30> Zarate/Berg				
10:00			10:00> COPPOLA / J Mitchell			
10:30					10:30> Inati	
11:00				11:00> Inati/Scott		11:00> COPPOLA / J Mitchell
11:30			11:30> Zarate/Berg			
12:00						
12:30						
13:00						
13:30						13:30> COPPOLA / J Mitchell
14:00		14:00> Zarate/Banerjee	14:00> COPPOLA / J Mitchell	14:00> Zarate/Lundin		
14:30						
15:00					15:00> Zarate/Lundin	
15:30						
16:00			16:00> He / Maniscalco	16:00> Maintenance		
16:30						16:30> He / Maniscalco
17:00						
17:30					17:30> Grillon/Balderston	
18:00						
18:30						
19:00						
19:30						
20:00						
20:30						20:30> Zarate/Berg

Adaptive reconfiguration of fractal small-world human brain functional networks

Danielle S. Bassett^{†‡}, Andreas Meyer-Lindenberg^{†§}, Sophie Achard^{*}, Thomas Duke[‡], and Edward Bullmore^{*§}

19518–19523 | PNAS | December 19, 2006 | vol. 103 | no. 51

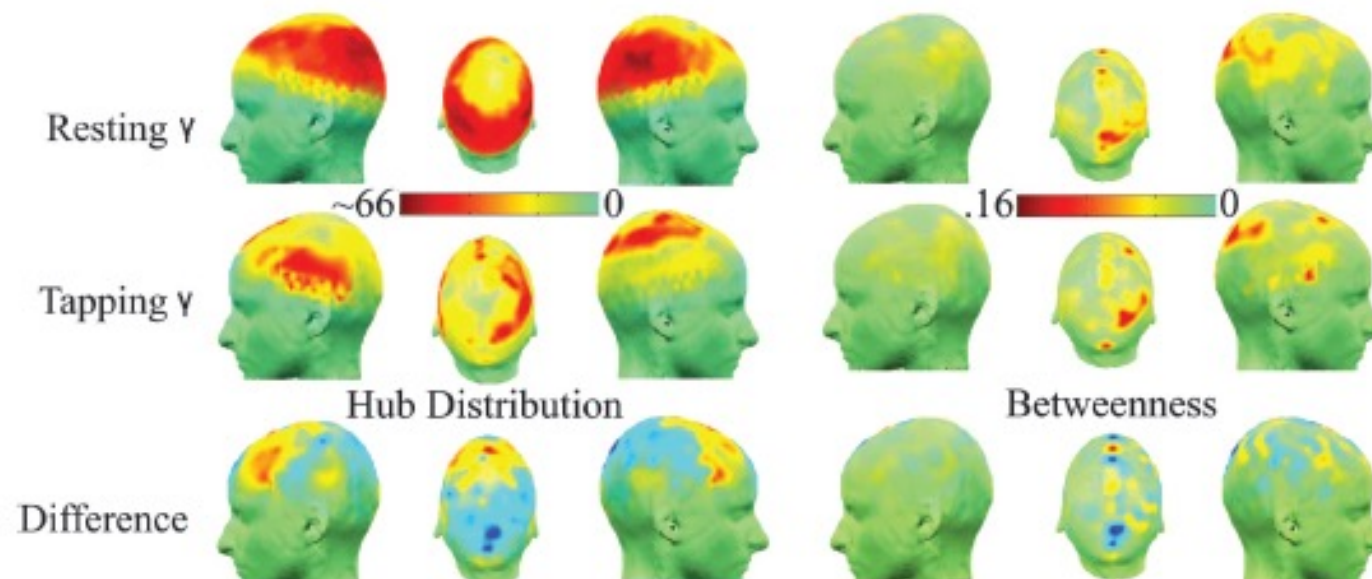
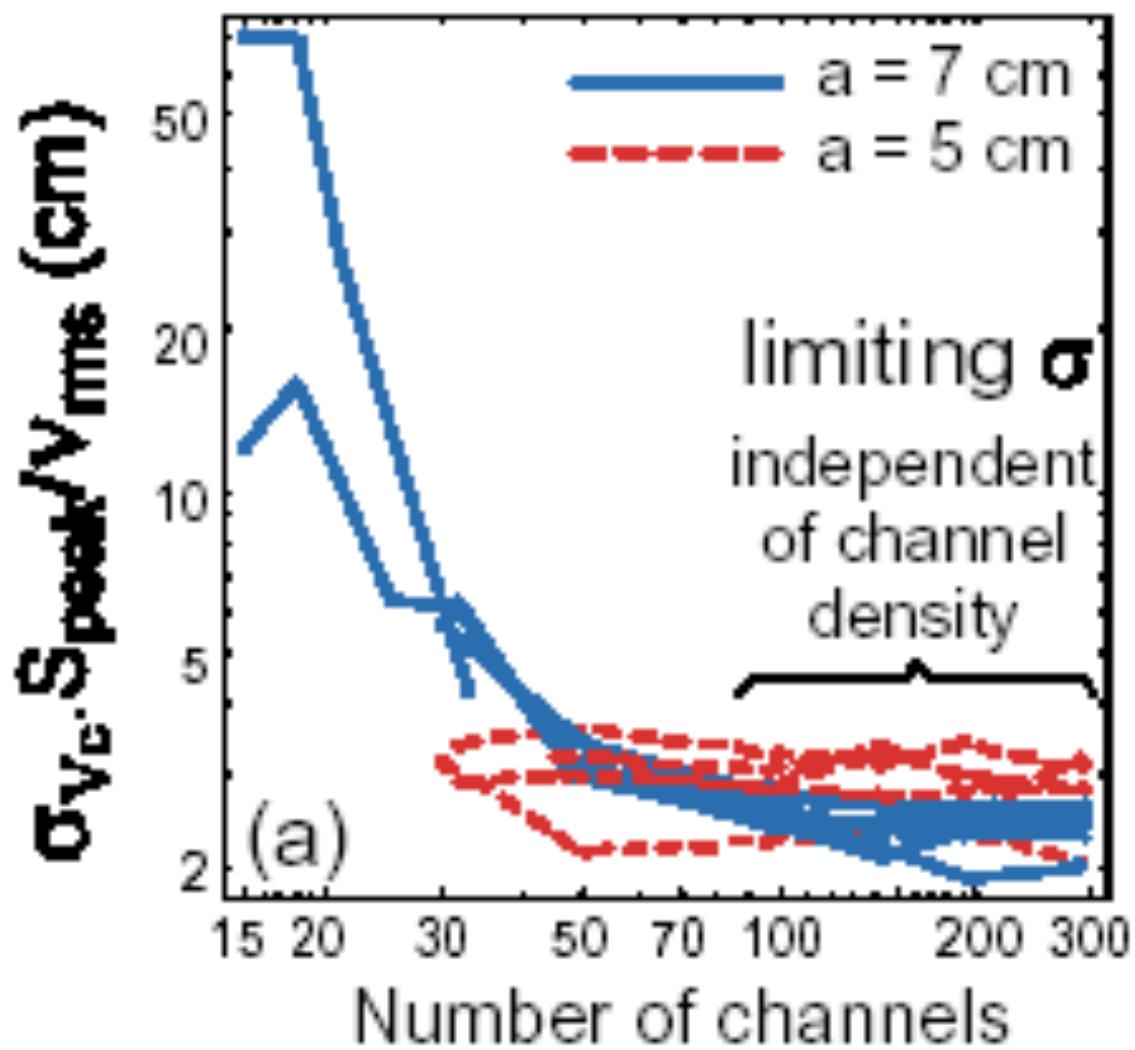


Fig. 3. State-related differences in spatial configuration of the highest frequency γ network. The top row shows the degree distribution and betweenness scores for the resting state γ network; the middle row shows the same maps for the motor γ network; the bottom row shows the between-state differences in degree and betweenness. It is clear that motor task performance is associated with emergence of greater connectivity in bilateral prefrontal and premotor nodes, and appearance of topologically pivotal nodes (with high betweenness scores) in medial premotor, right prefrontal, and parietal areas. See SI Fig. 7 for the betweenness distributions in both states at all frequency bands.

Dipole localization accuracy



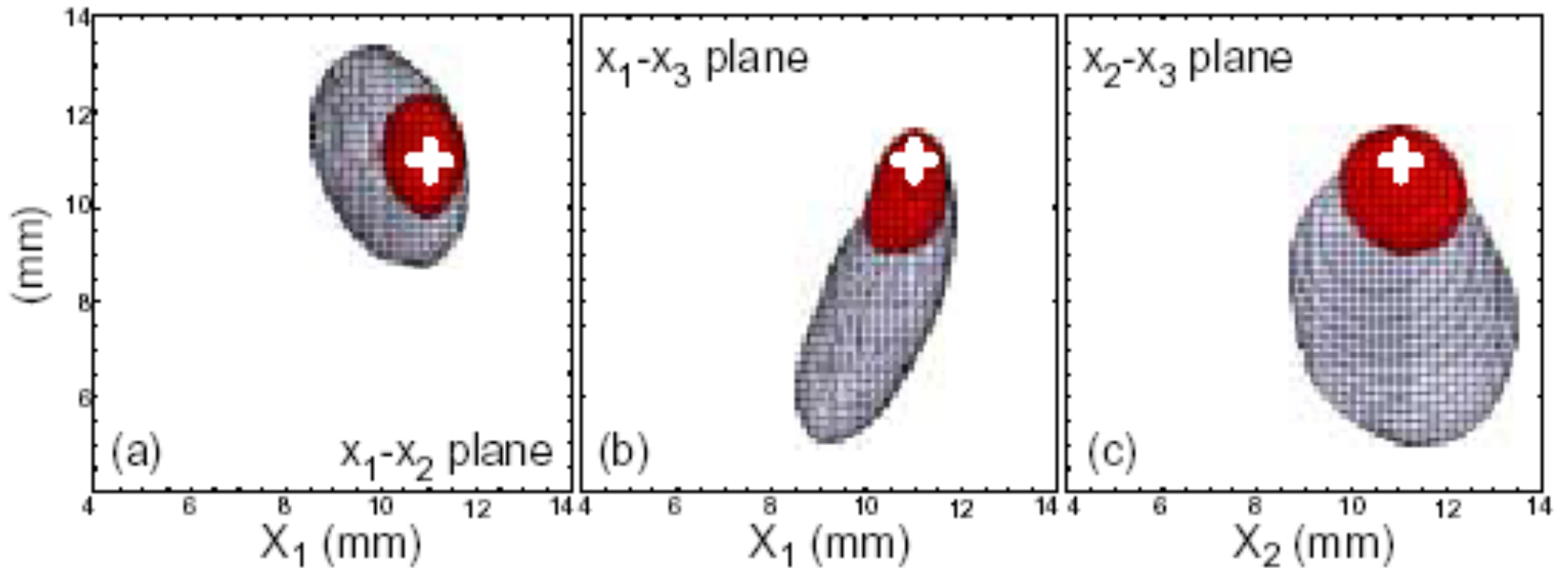
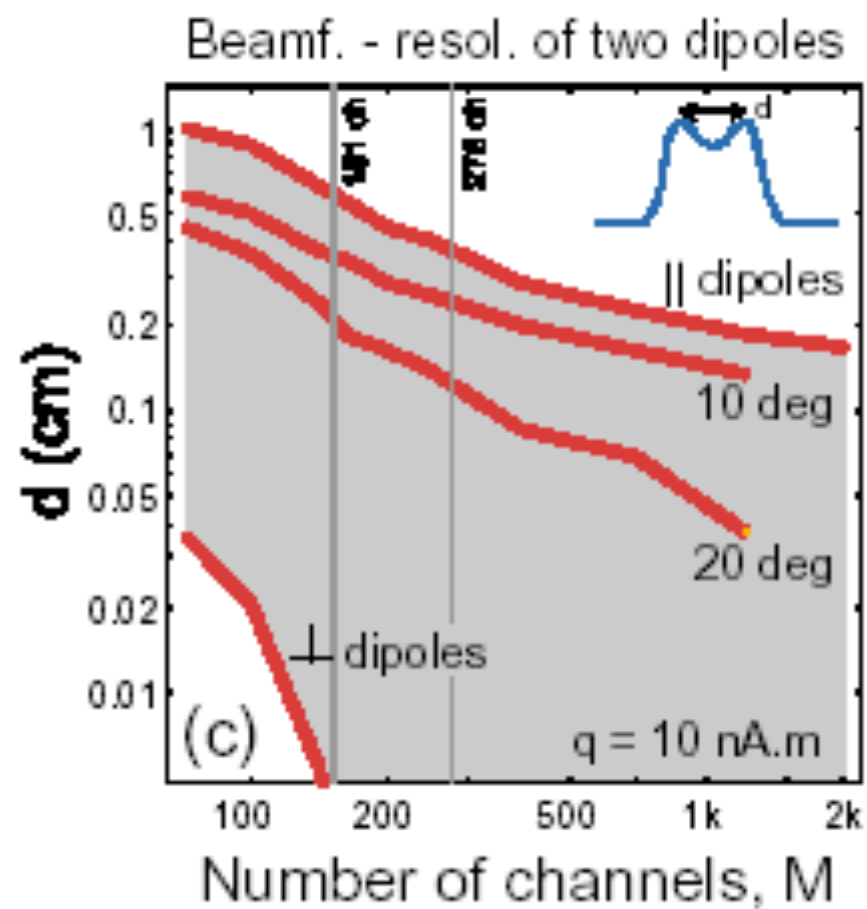
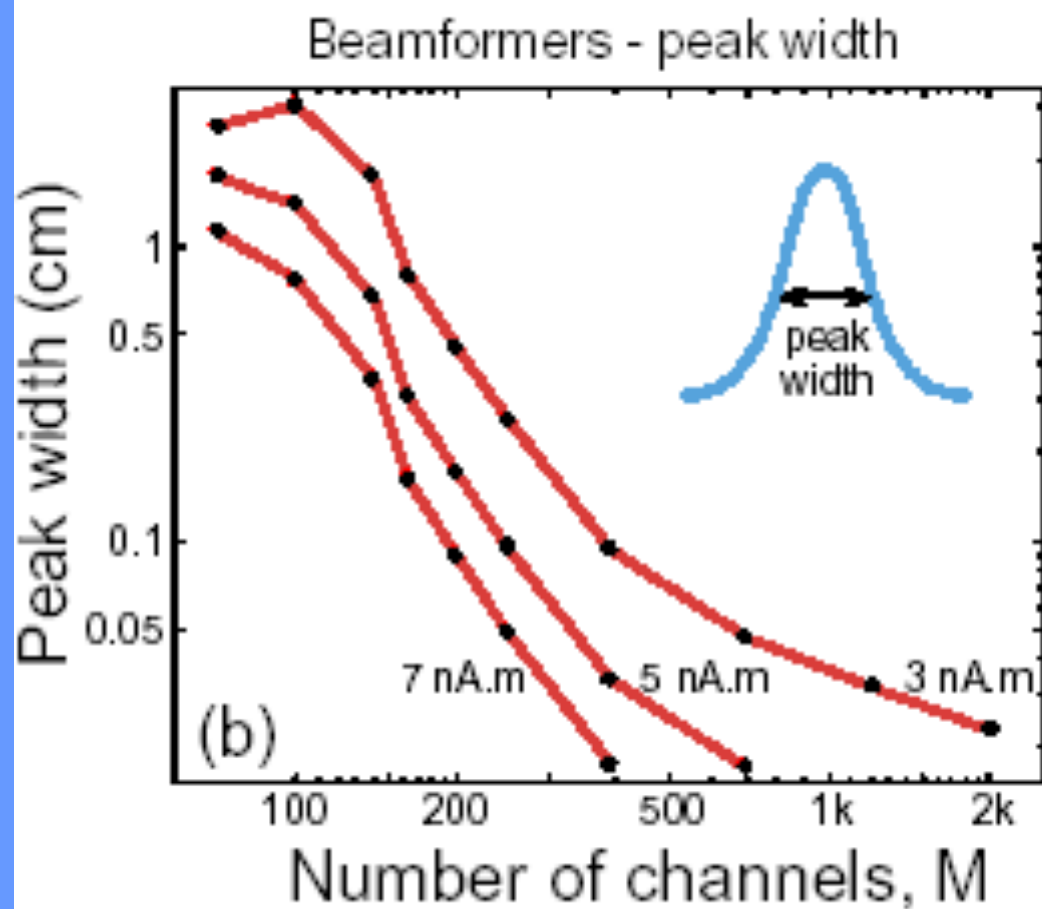


Fig.2: Benefit of increased channel number using measured brain and sensor noise in an unshielded environment with 3rd-order gradiometer noise cancellation. Dipole with 20 nA.m moment was inserted into measured brain noise, roughly 4.5 cm below the sensors. The half-amplitude 3D contours of normalized beamformer power are projected into x₁-x₂, x₁-x₃, and x₂-x₃ planes. White .+ . indicates the exact dipole position. Red shapes . 275 channel system, volume 6.1 mm³, gray shapes . 275 channel system resampled to 138 channels, volume 37.8 mm³



DipoleFit (Richard_SEF_20060606_05-av2.ds, none, richard-o.hdm)

File Edit Options Tools

Model Type:
 MEG
 EEG
 MEG+EEG
 Alpha: 0.50
 Update Moments Start Fit...

Dipole: 1 of 1
 Position: x = 1.06 cm, y = -5.51 cm, z = 8.56 cm
 Orientation: decl. = 70.65 deg, azim. = 37.14 deg
 constraint: none

Fit Type:
 Moving Dipole
 SpatioTemporal

Window Time(s) Sample
 Start: 0.0237 178
 End: 0.0237 178
 Width: 0.0000 1
 Trial: 1 of 3

Least-squares MEG only
 Iteration: 136
 Tot weighted err: 25.81 %
 Total MEG err: 25.81 %
 Total EEG err: 0.00 %

Cursor: Sample: 178
 Latency: 0.0237 s
 Weighted err: 25.81 %
 MEG err: 25.81 %
 EEG err: 0.00 %

Overlay All Channels Window Cursor Maps Home

MRI Viewer (richard-o.mri)

File Edit Options Tools Help

DIPOLE: Delete all dipoles
 1 of 5
 tr: 1, lat: 0.024s, err: 13.7%, st: good
 Display: All dipoles
 All marked
 Current slice only
 Current slice marked
 None
 Mark: Exclude bad
 Exclude error > 10.0 %

SAM SENSOR: Delete all sensors
 Delete current
 of 0 Edit ...

SAM PEAK: Delete all peaks
 Delete current
 of 0 Edit ...

Lock views to cursors
 GOTO: Nasion Right Ear
 Left Ear Sphere Origin

SPHERE:
 R(cm) X(cm) Y(cm) Z(cm)
 9.31 -1.56 0.27 4.57
 Fit to markers Fit to Headshape

DISPLAY: Brightness 50 Contrast 50

MARKER: Delete all markers
 Delete current
 of 0 Edit ...

Dipole File: fit5.dip

Dipoles

File Edit Options

Index	Trial	Sample	Latency(s)	Err.(%)	Good/Bad	Color	Mom(nAm)	xp(cm)	yp(cm)	zp(cm)	decl(deg)	azim(deg)	Label	Dataset
1	1	178	0.0237	13.6561	Good	Yellow	20.31	-0.937	-5.417	8.257	70.8	19.2	1	/home/coppolar/data/20060606/Richard_SEF_20060606_05_b1rmfix-av1.ds
2	1	178	0.0237	22.7785	Good	Yellow	11.23	-0.465	-6.101	8.677	75.7	19.1	2	/home/coppolar/data/20060606/Richard_SEF_20060606_05_b1rmfix-av2.ds
3	1	178	0.0237	5.9536	Good	Yellow	20.1	-0.726	-5.421	8.734	71.5	22.4	3	/home/coppolar/data/20060606/Richard_SEF_20060606_03-av.ds
4	1	178	0.0237	14.3576	Good	Yellow	20.42	-1.096	-5.354	8.263	70.2	18.3	4	/home/coppolar/data/20060606/Richard_SEF_20060606_05-av1.ds
5	1	178	0.0237	25.8065	Good	Yellow	10.89	1.057	-5.51	8.563	70.7	37.2	5	/home/coppolar/data/20060606/Richard_SEF_20060606_05-av2.ds